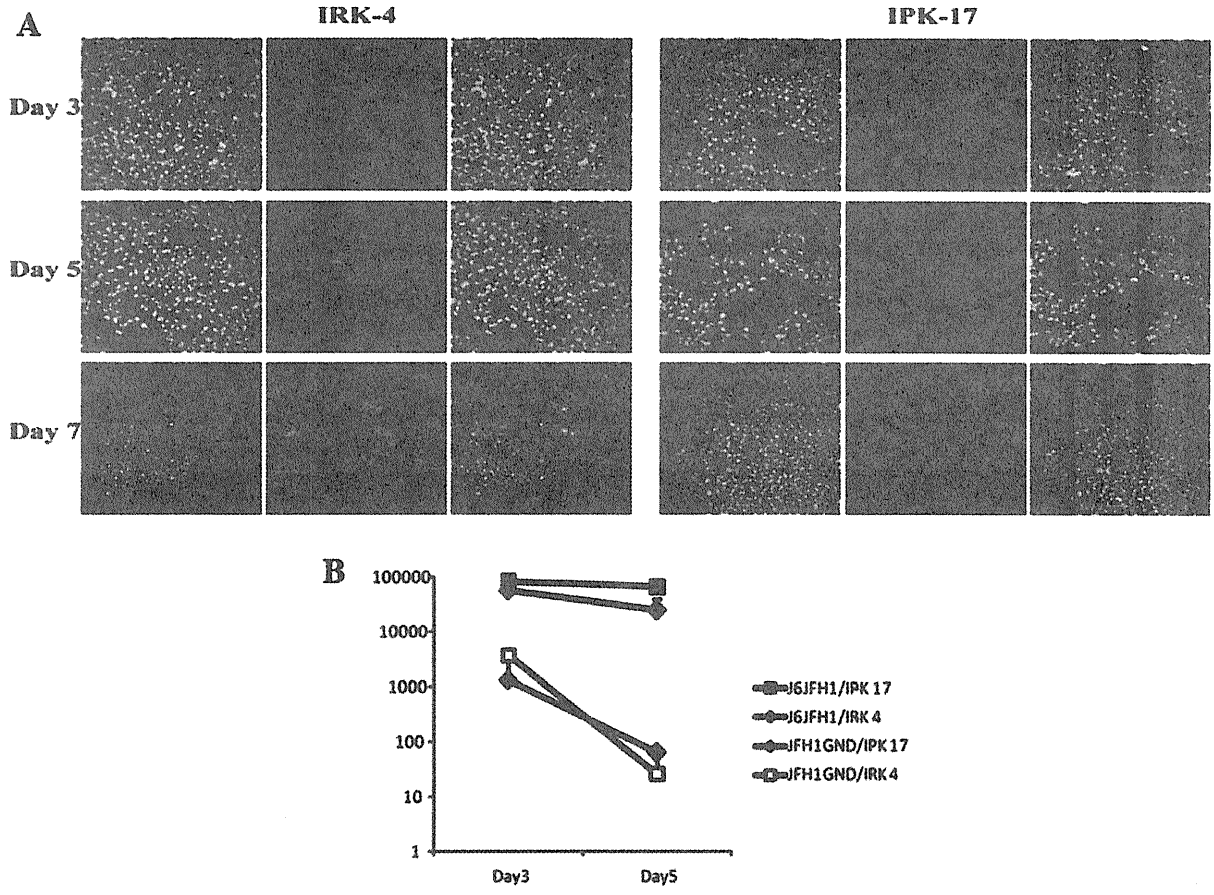


**Figure 3. Proliferation of HCV in IRK4 and IPK17 cells over time as detected by immunofluorescence staining of NS5a protein using the CL1 rabbit polyclonal antibody (A) and by quantitative real-time RT-PCR analysis of HCV-RNA levels (B).** JFH1GND was used as a negative control to exclude non replicating HCV-RNA. The data plotted represent the average +/− STD of 3 different experiments.
doi:10.1371/journal.pone.0021284.g003

## Discussion

Gene silencing of either IPS-1 or IFNAR significantly improves HCV replication and persistence in mouse hepatocytes compared with wild-type or TICAM-1ko mice. This result demonstrated the importance of the IPS-1 pathway rather than the TICAM-1 pathway in the induction of type I IFN by HCV infection, and revealed that the IFNAR amplification pathway confers resistance to HCV in mouse hepatocytes independently of TICAM-1. In accordance with our data, HCV-NS3/4A protease is known to cleave the IPS-1 and/or RIG-I-complement molecules including DDX3 and Riplet in humans to overcome the host innate immune response, showing the importance of RIG-I/IPS-1 pathway suppression in the establishment of HCV infection [10,11,12].

To further study factors affecting the HCV life cycle in mouse hepatocytes, we established IPK and IRK immortalized mouse hepatocyte lines by transduction with SV40T antigen. The established hepatocytes cell lines showed expression of HNF4, a major hepatocyte transcription factor, required for hepatocyte differentiation and liver-specific gene expression [13]. The maintenance of hepatocellular functions was demonstrated by continuous expression of hepatocyte specific differentiation marker, albumin, and the lack of expression of the bile duct marker, cytokeratin. The close resemblance of these cell lines to primary mouse hepatocytes is crucial to ensure the physiological relevance of factors identified in these cell lines that affect the HCV life cycle.

It is worth noting that HCV replication in IPS-1ko was higher than that in IFNARko hepatocytes. Since IPS-1 is present upstream of IFNAR in the IFN-amplification pathway, this higher J6JFH1 replication efficiency in IPS-1ko hepatocytes suggested the presence of an additive factor affecting HCV replication other than the induction of IFNAR-mediated type I IFN. This enhanced replication efficiency was also not accompanied by the induction of other interferon types, but was correlated with the reduction of HCV-induced apoptosis in mouse hepatocytes. This data clearly demonstrates that IPS-1 is playing an important role in the regulation of HCV infection in mouse hepatocytes through two different pathways, the IFN-induction pathways and another new IFN-independent pathway, leading to apoptotic cell death and elimination of HCV-harboring hepatocytes. The cytopathic effect of HCV infection in human cells is still contradictory. Although, some reports showed the induction of apoptosis and cell death by HCV infection in human hepatocytes [14,15,16], others showed suppression of apoptosis by HCV proteins [17,18]. This difference may be due to the different cell lines used in the different studies. Almost all the studies reporting HCV-induced apoptosis used

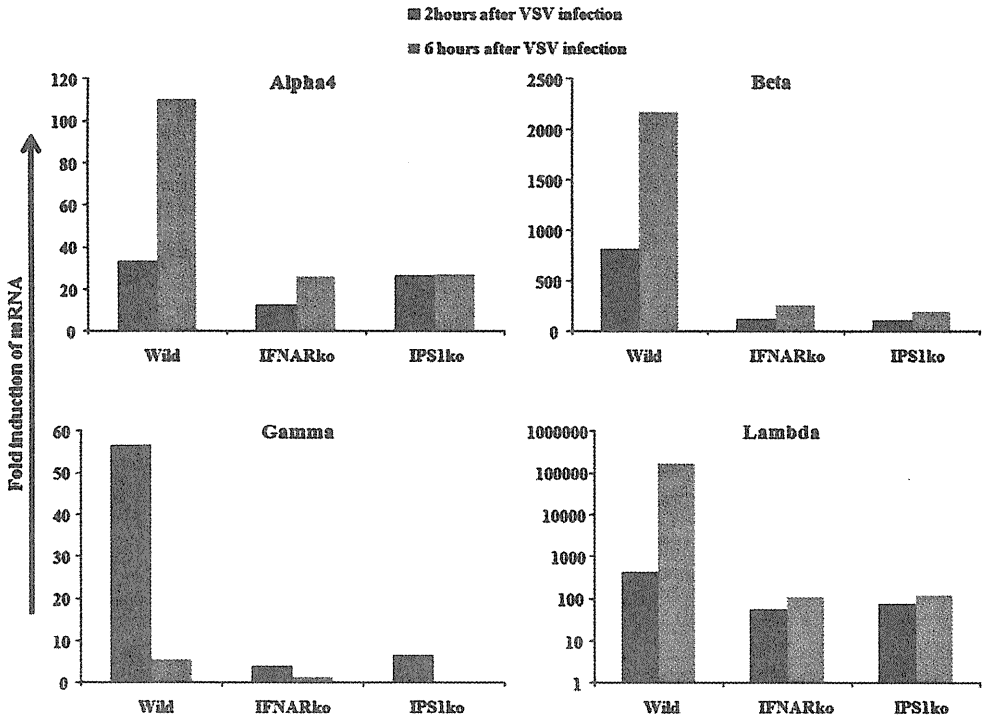


**Figure 4. Wild type, IFNARko, and IPS-1ko mice hepatocytes were infected with mock or VSV virus, 2 and 6 hours later, total RNA was extracted from the cells, and interferon alpha, beta, gamma and lambda mRNA induction levels were measured by real-time RT-PCR.** Similar results were obtained from 2 different experiments, each was performed in duplicates. The data plotted represent the mean duplicate readings in one of them.
doi:10.1371/journal.pone.0021284.g004

hepatocellular carcinoma cell lines. Since it has been established that the inability to undergo apoptosis is essential for the development of cancer [19,20,21], our use of immortalized, non-cancerous hepatocytes may make it possible to reproduce the physiological response of the cells to HCV infection more closely. The IPS-1 regulation of cell death following the introduction of HCV-RNA may also regulate the effector cell function. It is likely that hepatocyte debris generated secondary to intrinsic production of viral dsRNA in HCV-infected hepatocytes affect the antiviral effector response of the immune system through maturation of dendritic cells [22]. Hence, the effector cell activation may be enhanced by the induction of cell death through the IPS-1 pathway in hepatocytes which may facilitate producing dsRNA-containing debris.

In comparison to the JFH1GND construct with deficient replication that showed a rapid reduction in its RNA levels over time after transfection into mouse hepatocytes, J6JFH1 RNA was detected at four-log higher levels and was maintained at a relatively stable levels in IPS-1ko hepatocytes. Although the number of mouse cells expressing HCV proteins was found to increase over time, as detected by IF, the ratio between HCV-negative and -positive cells did not show any significant change for 7 days after transfection and increased after 10 days (data not shown). This indicates a negative selection of HCV-bearing cells over time which may be due to slower cellular replication, or loss of HCV replication. Another possibility may be that HCV infection is affected by the presence of an inhibitory factor possibly triggered by HCV replication or the lack of a human host factor required for HCV replication. Due to the initial replication of HCV in the transfected IPK and IRK mouse hepatocytes for the first 7 days and the establishment of infection, we favor the presence of a possible inhibitory factor that may be triggered by HCV replication. Another factor that also limits HCV spread in mouse hepatocytes is the failure of HCV to produce infectious particles in these cells (data no shown).

Using this newly established immortalized mouse hepatocyte line, we found that although J6JFH1, JFH1FL and the subgenomic JFH1 replicon all share a similar non-structural region derived from isolate JFH1 that is required for HCV replication, and although all of these constructs can replicate efficiently in HuH7.5.1 cells, strikingly, only J6JFH1 carrying the J6 structural region replicated in mouse hepatocytes. This indicates the importance of the J6 structural region and/or the chimeric construct between J6 and JFH1 for HCV replication in mouse hepatocytes. Structural regions are known to be important for HCV entry and/or particle formation [23], but this is the first time that their importance in replication in HCV-bearing cells has been demonstrated. This finding clearly shows the importance of non-hepatoma cell lines with less genetic abnormalities and mutations for the discovery of new aspects of the life cycle of HCV.

Although, the co-expression of human CD81 and Occludin genes was found to be important for HCVpp entry into murine NIH3T3 cells [3], the expression of hCD81 alone was sufficient for J6JFH1 entry into mouse hepatocytes. This may be explained by the different cell lines used in the different studies. In contrast to NIH3T3 cells, we used immortalized hepatocytes that showed close physiological resemblance to primary mouse hepatocytes and showed the expression of all the mouse counterparts of HCV entry

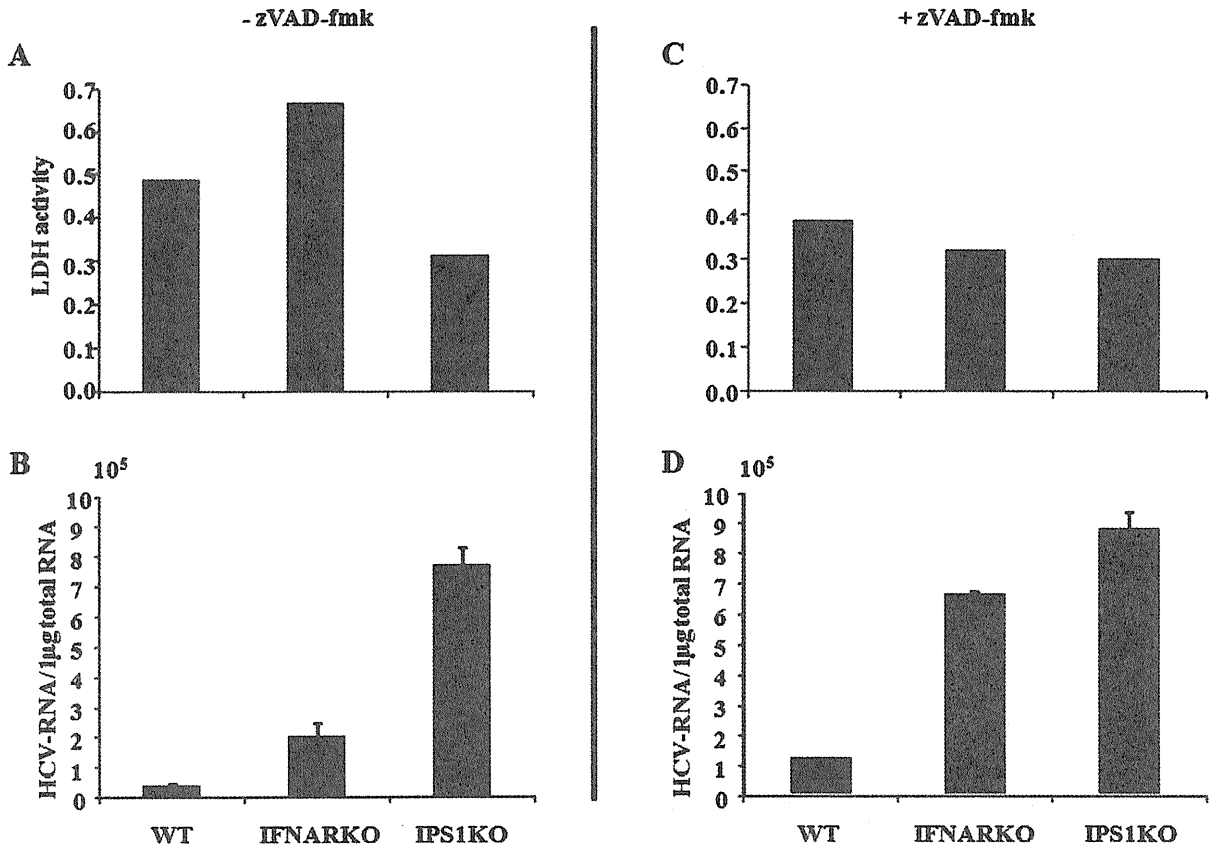


**Figure 5. Measurement of J6JFH1 mediated cytopathic effect in wild type, IFNARko, and IPS-1ko mouse hepatocytes.** Cultrure medium were left untreated (A;B) or treated with 20 μM of zVAD-fmK (C;D) 2 days before and after J6JFH1-RNA transfection. One day after transfection of J6JFH1-RNA, culture medium was discarded and cells were washed with PBS. A new medium was added and cells were cultured for another 24 hours. The LDH activity in the culture medium was measured in 2 different experiments in duplicates and showed similar results, the average levels of a duplicate from a single experiment was plotted (A, C). HCV-RNA titers in the cells were also measured using real-time RT-PCR (B, D), the data shown represent the mean +/− STD of 3 different experiments.
doi:10.1371/journal.pone.0021284.g005

receptors. A study from a different group showed that adaptive mutations in HCV envelope proteins allowing its interaction with murine CD81 is enough for efficient HCVpp entry without the expression of any human entry receptors in murine cells [24]. This report, together with ours, suggest that CD81 is the main human host restriction factor for HCV entry, and that overcoming this problem either by HCV adaptation to murine CD81, or the expression of human CD81 in murine hepatocytes is essential for HCV entry. Although our lentivirus transfection efficiency with CD81 was around 95% in IPK and IRK clones, only 1% of the cells were prone to infection with HCVcc. Also, HCVpp showed lower entry levels in those cells compared to HuH7.5.1 cells (Fig. S6). This suggests that hCD81 expression is the minimum and most crucial requirement for HCV entry into mouse hepatocytes. The discovery and expression of other co-receptors facilitating HCV entry in human cells is still required for efficient and robust HCV infection.

In summary, the suppression of IPS-1 is important for the establishment of HCV infection and replication in mouse hepatocytes through the suppression of both interferon induction and interferon independent J6JFH1-induced cytopathic effect. We have established hepatocytes lines from IPS-1 and IFNARko mice that support HCV replication and infection. These cell lines will be very useful in identifying other species restriction factors and viral determinants required for further establishment of a robust and efficient HCV life cycle in mouse hepatocytes. Using those cells, we showed for the first time the importance of HCV structural region for viral replication. IRF3ko mouse embryo fibroblasts (MEFs) were previously shown to support HCV replication more efficiently than wild MEFs [25]. Since the knockout of IPS-1 mainly suppresses signaling in response to virus RNA detection, and maintains an intact IFN response to other stimulants, it may result in minimum interference to adaptive immune responses as compared to IRF3 or IFNARko. Therefore, further development of hCD81-transgenic IPS-1ko mice may serve as a good model for the study of immunological responses against HCV infection. This mouse model can be used as a backbone for any further future models supporting robust HCV infectivity for the study of HCV pathogenesis, propagation and vaccine development.

## Material and Methods

### Cell culture

HuH7.5.1 cells were cultured in high-glucose Dulbecco's modified Eagle's medium (DMEM; Gibco/Invitrogen, Tokyo, Japan) supplemented with 2 mM L-glutamine, 100 U of penicillin/ml, 100 μg of

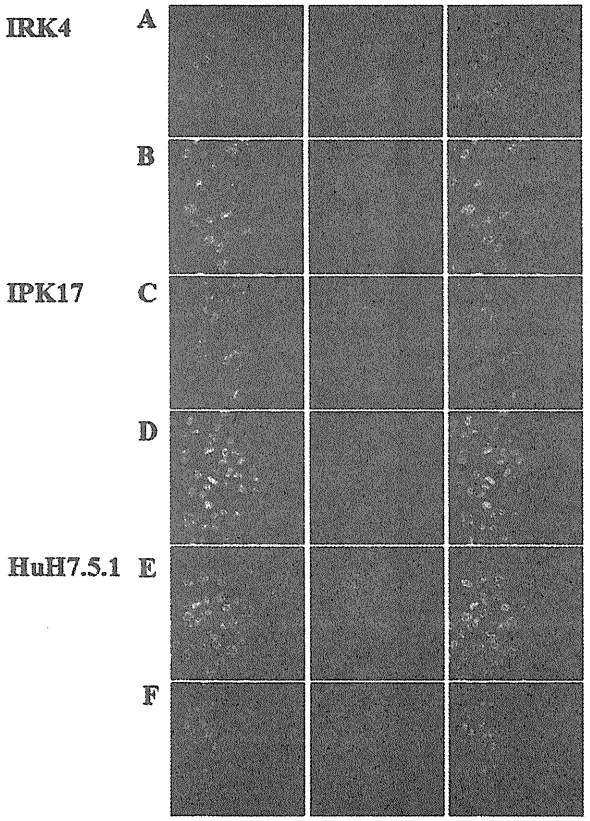


**Figure 6. J6JFH1 infection into IRK-4 and IPK17 cells. HCV-NS5A protein detection in mouse IRK4 (A,B) and IPK17 (C,D) and human 7.5.1 cells (E,F).** The cells were transduced with lentivirus expressing human CD81 gene at 10 MOI. 48 hours later the cells were infected with 100 times concentrated supernatant medium, collected during 1 week after transfection of HuH7.5.1 cells with J6JFH1-RNA (A, C, and E) or JFH1GND-RNA (B, D, and F).
doi:10.1371/journal.pone.0021284.g006

streptomycin/ml and 10% fetal bovine serum. Mouse primary hepatocytes were isolated from the liver using collagenase perfusion through the inferior vena cava (IVC), while clamping the animal's intrathoracic extension. Hepatocyte isolation and perfusion control were performed as previously described [26]. Primary and immortalized hepatocytes were cultured in a similar medium supplemented with: HEPES (Gibco/Invitrogen), 20 mmol/L; L-proline, 30 μg/mL; insulin (Sigma, St. Louis, MO, USA), 0.5 μg/mL; dexamethasone (Wako, Osaka, Japan), $1\times10^{-7}$ mol/L; $NaHCO_3$, 44 mmol/L; nicotinamide (Wako), 10 mmol/L; EGF (Wako), 10 ng/mL; L-ascorbic acid 2-phosphate (Wako), 0.2 mmol/L; and MEM-non essential amino acids (Gibco/Invitrogen), 1%.

## Gene-disrupted mice

All mice were backcrossed with C57BL/6 mice more than seven times before use. Toll-like receptor adaptor molecule 1 (TICAM-1) ko [27] and IPS-1ko mice [28] were generated in our laboratory (detailed information regarding the IPS-1 mice will be presented elsewhere). All mice were maintained under specific-pathogen-free conditions in the animal facility of the Hokkaido University Graduate School of Medicine (Japan).

## RNA extraction, reverse transcriptase polymerase chain reaction (RT-PCR) and real-time RT-PCR

RNA was extracted from cultured cells using Trizol reagent (Invitrogen, San Diego, CA, USA) according to the manufacturer's protocol. Using 1 μg of total RNA as a template, we performed RT-PCR and real-time RT-PCR as previously described [29,30].

## *In vitro* RNA transcription, transfection and preparation of J6JFH1 and Jfh1 viruses

*In vitro* RNA transcription, transfection into HuH7.5.1 or mouse hepatocytes, and preparation of J6JFH1 and JFH1 viruses, were all performed as previously reported [31]. RNA transfection into human and mouse hepatocytes was performed by electroporation using a Gene Pulser II (Bio-Rad, Berkeley, California) at 260 V and 950 Cap.

## HCV infection

J6JFH1 and JFH1 concentrated medium were adjusted to contain a similar RNA copy number by real-time RT-PCR. $2\times10^4$ cells/well were cultured in 8-well glass chamber slides. After 24 hours, the medium was removed and replaced by concentrated medium containing JFH1 or J6JFH1 viruses. After three hours, the concentrated medium was removed, cells were washed with PBS and incubated in fresh medium for 48 hours, before the detection of infection.

## Lentivirus construction, titration and infection

The gene encoding T antigen from simian virus was cloned from plasmid CSII-EF-SVT [32]. The genes encoding human CD81 and occludin were cloned from HuH-7.5.1 cells using the Zero Blunt TOPO PCR Cloning Kit (Invitrogen) according to the manufacturer's protocol. These genes were then inserted into the GFP reporter gene-containing lentiviral expression (pLBIG) vector using the *Eco*RI and *Xho*I restriction sites for SV40T and hCD81, and the *Xba*I and *Xho*I restriction sites for hOccludin. Lentivirus expression vectors were then constructed as previously described [27]. GFP expression was used for the titration of lentivirus vectors, and a multiplicity of infection (MOI) of 10 was used for the infection of mouse cells. Forty-eight hours after the transfection of hCD81 and/or hOccludin, cells were trypsinized and counted. Then, $2\times10^4$ cells/well were cultured in 8-well glass chamber slides for HCV infection and $5\times10^4$ cells/well were cultured in 12-well plates, along with 1 ml of medium containing HCVpp, for HCV entry experiments.

## HCVpp construction and the detection of luciferase expression

HCVpp containing the E1 and E2 proteins from HCV isolate J6 and expressing the luciferase reporter gene were a kind gift from Dr. Thomas Pietschmann at the TWINCORE Center for Experimental and Clinical Infection Research, Germany. The production of HCVpp and the measurement of luciferase levels were performed as previously described [33].

## Indirect immunofluorescence (IF)

IF expression of HCV proteins was detected in the infected cells using antibodies in the serum of chronic HCV patients or rabbit IgG anti-NS5A antibody (Cl-1) (both kind gifts from K. Shimotohno, Chiba Institute of Technology, Japan). Goat anti-human IgG Alexa 594 and goat anti-rabbit Alexa 594 (Invitrogen) were used as secondary antibodies, respectively. Fluorescence

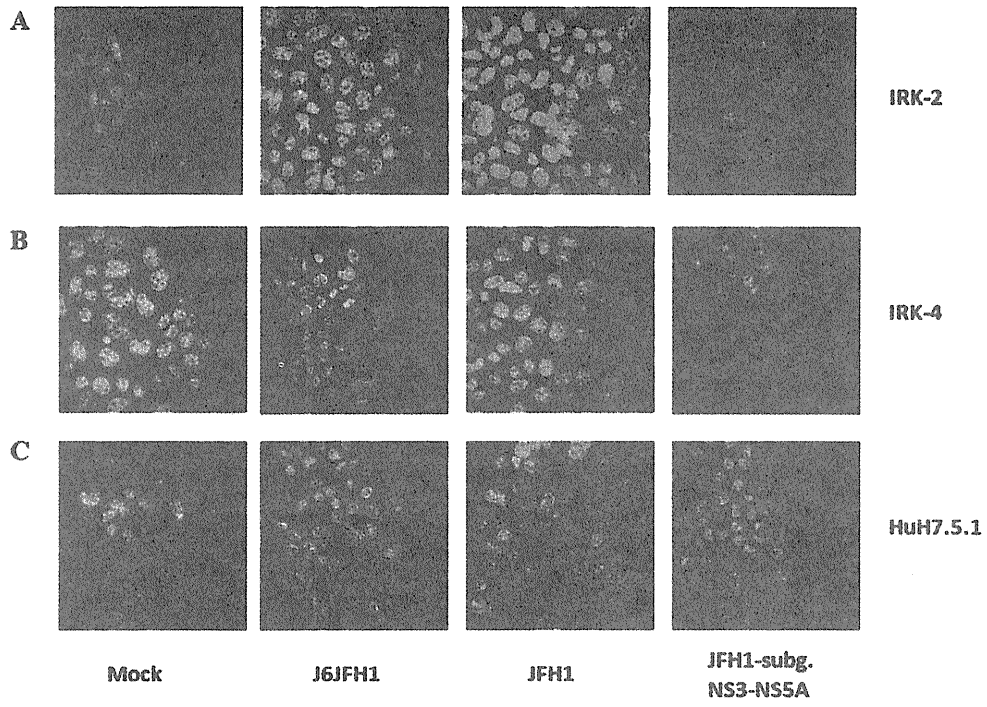


**Figure 7. Detection of HCV-NS5A protein in IRK-2 (A), IRK-4 (B) and HuH-7.5 cells (C) by IF 5 days after transfection with J6JFH1, FL-JFH1 or subgenomic JFH1-RNA.**
doi:10.1371/journal.pone.0021284.g007

detection was performed on a ZEISS LSM 510 Meta confocal microscope (Zeiss, Jena, Germany).

### Detection of cell death

Culture medium was collected from HCV infected and control cells and used for measuring lactate dehydrogenase (LDH) levels using an LDH cytotoxicity detection kit (Takara Biomedicals, Tokyo, Japan). Light absorbance was then measured according to the manufacturer's protocol.

### Ethic Statement

This study was carried out in strict accordance with the recommendations in the Guide for the Care and Use of Laboratory Animals of the National Institutes of Health. The protocol was approved by the Committee on the Ethics of Animal Experiments in the Animal Safety Center, Hokkaido University, Japan. All mice were used according to the guidelines of the institutional animal care and use committee of Hokkaido University, who approved this study as ID number: 08-0243, " Analysis of immune modulation by toll-like receptors".

## Supporting Information

**Figure S1** RT detection of TLR3, TLR7, RIG-I, and IPS-1 expression in mouse hepatocytes. GAPDH expression was used as internal control, and RNA from CD11c+ spleenocytes (dendritic cells) was used as positive control.
(TIF)

**Figure S2** Proliferation of HCV in IPS-1, TICAM-1(TRIF) and IFNAR-knockout mouse hepatocytes over time as detected by quantitative real-time RT-PCR analysis of HCV-RNA levels. JFH1GND transfection into IPS-1 knockout cells was used as a negative control to exclude non replicating HCV RNA. The data plotted represent the average +/− STD of 3 different experiments.
(TIF)

**Figure S3** RT detection of CD81, Occludin, Claudin 1, SRB1, and LDL receptor expression in primary, IRK4 and IPK17 mouse hepatocytes. GAPDH expression was used as internal control.
(TIF)

**Figure S4** Estimation of the transfection efficiency of lentivirus vector expressing green fluorescent protein (GFP) as a reporter, together with hCD81 or hOccludin. 48 hours after transfection with the lentivirus vector, cells were trypsinized and GFP positive cells were detected by BD FACSCalibur (BD Biosciences).
(TIF)

**Figure S5** HCV infection of IRK2 cells transfected with lentivirus expressing hCD81 and/or hOccludin. IRK2 cells were transfected with lentivirus expressing empty vector (A), hCD81 (B), hOccludin (C) or hCD81 and hOccludin (D) at a MOI of 10. After 48 hours, the cells were infected with concentrated J6JFH1 transfected 7.5.1 culture medium. After a further three hours, cells were washed with PBS and incubated in fresh medium. After another 48 hours, HCV infection was examined through the detection of HCV-NS5a protein expression by immunofluorescence staining.
(TIF)

**Figure S6** HCVpp entry into mouse cells. A similar number of IPK17 and HuH7.5.1 were cultured in triplicate. IPK17 cells were only transfected with lentivirus expressing hCD81, while HuH7.5.1 cells were transfected with empty vector at a MOI of

10. After 48 hours, the medium was replaced with a new medium containing mock VSVG-pp or HCVpp expressing luciferase. After another 48 hours, pseudoparticles entry was determined by measuring the luciferase activity. In order to compare the HCVpp entry between IPK17 and HuH7.5.1 cells, the luciferase expression from VSV-Gpp entry was used an internal control, while that from HCVpp was plotted relatively.
(TIF)

## Acknowledgments

We want to thank Dr. Michinori Kohara (Tokyo Metropolitan Institute for Medical Science, Tokyo, Japan); Dr. Tadatsugu Taniguchi (University of Tokyo, Yokyo, Japan); Dr. Thomas Pietschmann (Division of Experimental Virology, TWINCORE, Hannover, Germany); and Dr. Makoto Hijikata (The Institute for Virus Research, Kyoto University, Japan) for their generous supply of research material. Dr. Hussein H. Aly was supported by a JSPS postdoctoral fellowship from the Japan Society for the Promotion of Science.

## Author Contributions

Conceived and designed the experiments: HHA TS. Performed the experiments: HHA HO. Analyzed the data: HHA MM HO HS TS. Contributed reagents/materials/analysis tools: KS TW. Wrote the paper: HHA.

## References

1. Seto WK, Lai CL, Fung J, Hung I, Yuen J, et al. (2010) Natural history of chronic hepatitis C: Genotype 1 versus genotype 6. J Hepatol.
2. Uprichard SL, Chung J, Chisari FV, Wakita T (2006) Replication of a hepatitis C virus replicon clone in mouse cells. Virol J 3: 89.
3. Ploss A, Evans MJ, Gaysinskaya VA, Panis M, You H, et al. (2009) Human occludin is a hepatitis C virus entry factor required for infection of mouse cells. Nature 457: 882–886.
4. Diamond MS (2009) Mechanisms of evasion of the type I interferon antiviral response by flaviviruses. J Interferon Cytokine Res 29: 521–530.
5. O'Neill LA, Bowie AG (2010) Sensing and signaling in antiviral innate immunity. Curr Biol 20: R328–333.
6. Platanias LC (2005) Mechanisms of type-I- and type-II-interferon-mediated signalling. Nat Rev Immunol 5: 375–386.
7. Tanaka Y, Nishida N, Sugiyama M, Kurosaki M, Matsuura K, et al. (2009) Genome-wide association of IL28B with response to pegylated interferon-alpha and ribavirin therapy for chronic hepatitis C. Nat Genet 41: 1105–1109.
8. Thompson AJ, Muir AJ, Sulkowski MS, Ge D, Fellay J, et al. (2010) Interleukin-28B polymorphism improves viral kinetics and is the strongest pretreatment predictor of sustained virologic response in genotype 1 hepatitis C virus. Gastroenterology 139: 120–129. e118.
9. Sumpter R, Jr., Loo YM, Foy E, Li K, Yoneyama M, et al. (2005) Regulating intracellular antiviral defense and permissiveness to hepatitis C virus RNA replication through a cellular RNA helicase, RIG-I. J Virol 79: 2689–2699.
10. Foy E, Li K, Sumpter R, Jr., Loo YM, Johnson CL, et al. (2005) Control of antiviral defenses through hepatitis C virus disruption of retinoic acid-inducible gene-I signaling. Proc Natl Acad Sci U S A 102: 2986–2991.
11. Oshiumi H, Ikeda M, Matsumoto M, Watanabe A, Takeuchi O, et al. (2010) Hepatitis C virus core protein abrogates the DDX3 function that enhances IPS-1-mediated IFN-beta induction. PLoS One 5: e14258.
12. Oshiumi H, Miyashita M, Inoue N, Okabe M, Matsumoto M, et al. (2010) The ubiquitin ligase Riplet is essential for RIG-I-dependent innate immune responses to RNA virus infection. Cell Host Microbe 8: 496–509.
13. Ishiyama T, Kano J, Minami Y, Iijima T, Morishita Y, et al. (2003) Expression of HNFs and C/EBP alpha is correlated with immunocytochemical differentiation of cell lines derived from human hepatocellular carcinomas, hepatoblastomas and immortalized hepatocytes. Cancer Sci 94: 757–763.
14. Berg CP, Schlosser SF, Neukirchen DK, Papadakis C, Gregor M, et al. (2009) Hepatitis C virus core protein induces apoptosis-like caspase independent cell death. Virol J 6: 213.
15. Deng L, Adachi T, Kitayama K, Bungyoku Y, Kitazawa S, et al. (2008) Hepatitis C virus infection induces apoptosis through a Bax-triggered, mitochondrion-mediated, caspase 3-dependent pathway. J Virol 82: 10375–10385.
16. Zhu H, Dong H, Eksioglu E, Hemming A, Cao M, et al. (2007) Hepatitis C virus triggers apoptosis of a newly developed hepatoma cell line through antiviral defense system. Gastroenterology 133: 1649–1659.
17. Ray RB, Meyer K, Ray R (1996) Suppression of apoptotic cell death by hepatitis C virus core protein. Virology 226: 176–182.
18. Mankouri J, Dallas ML, Hughes ME, Griffin SD, Macdonald A, et al. (2009) Suppression of a pro-apoptotic K+ channel as a mechanism for hepatitis C virus persistence. Proc Natl Acad Sci U S A 106: 15903–15908.
19. Ladu S, Calvisi DF, Conner EA, Farina M, Factor VM, et al. (2008) E2F1 inhibits c-Myc-driven apoptosis via PIK3CA/Akt/mTOR and COX-2 in a mouse model of human liver cancer. Gastroenterology 135: 1322–1332.
20. Lowe SW, Lin AW (2000) Apoptosis in cancer. Carcinogenesis 21: 485–495.
21. Schulze-Bergkamen H, Krammer PH (2004) Apoptosis in cancer--implications for therapy. Semin Oncol 31: 90–119.
22. Ebihara T, Shingai M, Matsumoto M, Wakita T, Seya T (2008) Hepatitis C virus-infected hepatocytes extrinsically modulate dendritic cell maturation to activate T cells and natural killer cells. Hepatology 48: 48–58.
23. Mateu G, Donis RO, Wakita T, Bukh J, Grakoui A (2008) Intragenotypic JFH1 based recombinant hepatitis C virus produces high levels of infectious particles but causes increased cell death. Virology 376: 397–407.
24. Bitzegeio J, Bankwitz D, Hueging K, Haid S, Brohm C, et al. (2010) Adaptation of hepatitis C virus to mouse CD81 permits infection of mouse cells in the absence of human entry factors. PLoS Pathog 6: e1000978.
25. Lin LT, Noyce RS, Pham TN, Wilson JA, Sisson GR, et al. (2010) Replication of subgenomic hepatitis C virus replicons in mouse fibroblasts is facilitated by deletion of interferon regulatory factor 3 and expression of liver-specific microRNA 122. J Virol 84: 9170–9180.
26. Ishigami A, Fujita T, Handa S, Shirasawa T, Koseki H, et al. (2002) Senescence marker protein-30 knockout mouse liver is highly susceptible to tumor necrosis factor-alpha- and Fas-mediated apoptosis. Am J Pathol 161: 1273–1281.
27. Akazawa T, Ebihara T, Okuno M, Okuda Y, Shingai M, et al. (2007) Antitumor NK activation induced by the Toll-like receptor 3-TICAM-1 (TRIF) pathway in myeloid dendritic cells. Proc Natl Acad Sci U S A 104: 252–257.
28. Ebihara T, Azuma M, Oshiumi H, Kasamatsu J, Iwabuchi K, et al. (2010) Identification of a polyI:C-inducible membrane protein that participates in dendritic cell-mediated natural killer cell activation. J Exp Med 207: 2675–2687.
29. Aly HH, Qi Y, Atsuzawa K, Usuda N, Takada Y, et al. (2009) Strain-dependent viral dynamics and virus-cell interactions in a novel in vitro system supporting the life cycle of blood-borne hepatitis C virus. Hepatology 50: 689–696.
30. Aly HH, Shimotohno K, Hijikata M (2009) 3D cultured immortalized human hepatocytes useful to develop drugs for blood-borne HCV. Biochem Biophys Res Commun 379: 330–334.
31. Wakita T, Pietschmann T, Kato T, Date T, Miyamoto M, et al. (2005) Production of infectious hepatitis C virus in tissue culture from a cloned viral genome. Nat Med 11: 791–796.
32. Aly HH, Watashi K, Hijikata M, Kaneko H, Takada Y, et al. (2007) Serum-derived hepatitis C virus infectivity in interferon regulatory factor-7-suppressed human primary hepatocytes. J Hepatol 46: 26–36.
33. Haid S, Windisch MP, Bartenschlager R, Pietschmann T (2010) Mouse-specific residues of claudin-1 limit hepatitis C virus genotype 2a infection in a human hepatocyte cell line. J Virol 84: 964–975.

JOURNAL OF VIROLOGY, June 2011, p. 5423–5435 Vol. 85, No. 11
0022-538X/11/$12.00 doi:10.1128/JVI.02146-10
Copyright © 2011, American Society for Microbiology. All Rights Reserved.

# Natural Killer Cells Recognize Friend Retrovirus-Infected Erythroid Progenitor Cells through NKG2D–RAE-1 Interactions *In Vivo*[▽]

Tatsuya Ogawa,[1,2]†§ Sachiyo Tsuji-Kawahara,[1]§ Takae Yuasa,[1] Saori Kinoshita,[1] Tomomi Chikaishi,[1,3] Shiki Takamura,[1] Haruo Matsumura,[1]‡ Tsukasa Seya,[4] Toshihiko Saga,[2] and Masaaki Miyazawa[1]*

*Department of Immunology[1] and Department of Cardiovascular Surgery,[2] Kinki University School of Medicine, Osaka-Sayama, Osaka, Japan; Unmet Medical Needs Pharma, Inc., Yokohama, Japan[3]; and Department of Microbiology and Immunology, Hokkaido University Graduate School of Medicine, Kita-ku, Sapporo 060-8638, Japan[4]*

Received 12 October 2010/Accepted 10 March 2011

**Natural killer (NK) cells function as early effector cells in the innate immune defense against viral infections and also participate in the regulation of normal and malignant hematopoiesis. NK cell activities have been associated with early clearance of viremia in experimental simian immunodeficiency virus and clinical human immunodeficiency virus type 1 (HIV-1) infections. We have previously shown that NK cells function as major cytotoxic effector cells in vaccine-induced immune protection against Friend virus (FV)-induced leukemia, and NK cell depletion totally abrogates the above protective immunity. However, how NK cells recognize retrovirus-infected cells remains largely unclear. The present study demonstrates a correlation between the expression of the products of retinoic acid early transcript-1 (RAE-1) genes in target cells and their susceptibility to killing by NK cells isolated from FV-infected animals. This killing was abrogated by antibodies blocking the NKG2D receptor *in vitro*. Further, the expression of RAE-1 proteins on erythroblast surfaces increased early after FV inoculation, and administration of an RAE-1-blocking antibody resulted in increased spleen infectious centers and exaggerated pathology, indicating that FV-infected erythroid cells are recognized by NK cells mainly through the NKG2D–RAE-1 interactions *in vivo*. Enhanced retroviral replication due to host gene-targeting resulted in markedly increased RAE-1 expression in the absence of massive erythroid cell proliferation, indicating a direct role of retroviral replication in RAE-1 upregulation.**

Natural killer (NK) cells play an important role in eliminating virus-infected cells via both direct killing and antibody-dependent cell-mediated cytotoxicity mechanisms (15, 49). NK cells also control adaptive immune responses through the production of key cytokines in the early stages of viral infection. In addition, NK cells have been implicated in the growth regulation of hematopoietic cells (6, 39). Thus, viruses that infect hematopoietic cells are prime targets of NK cells. In fact, NK cells are expanded and activated during acute human immunodeficiency virus type 1 (HIV-1) infection prior to seroconversion (1), and NK cell activity parallels changes in plasma viral load both in experimental infection of rhesus macaques with a pathogenic simian immunodeficiency virus isolate (10) and in clinical HIV-1 infection (21). Increased NK cell activities in high-risk HIV-1-exposed uninfected individuals (34, 38) also indicate a possible role of NK cells in resistance against HIV-1 acquisition. Genetic analyses of large cohorts have provided compelling evidence for correlations between certain haplotypes of the killer cell immunoglobulin-like receptor (KIR) loci and slow progression to AIDS after HIV-1 seroconversion (9, 23, 24), connecting NK cell activities with restricted HIV-1 replication. NK cells are also reduced in patients with human T-lymphotropic virus type 1 (HTLV-1)-associated disorders (3), indicating possible disease progression in the absence of NK cell-mediated virus control. However, little is known about the molecular mechanisms through which retrovirus-infected cells are recognized by NK cells.

Friend virus (FV) is a highly leukemogenic and immunosuppressive mouse retrovirus complex composed of replication-competent Friend murine leukemia virus (F-MuLV) and replication-defective but acutely transforming Friend spleen focus-forming virus (SFFV). The product of the SFFV *env* gene, gp55, forms a complex with the erythropoietin receptor and the short form of the hematopoietic cell-specific receptor tyrosine kinase (STK), and this interaction induces the growth and terminal differentiation of erythroid progenitor cells, causing polycythemia and massive splenomegaly (18, 28). The resultant increase in targets of FV integration consequently causes the emergence of mono- or oligoclonal erythroleukemia through insertional activation of transcription factors or disruption of a tumor suppressor gene. Since the above early splenomegaly and late erythroleukemogenesis can be induced by inoculating the virus into immunocompetent adult mice of susceptible strains, FV has contributed to the analysis of host immune responses that influence retrovirus replication and disease development (5, 12, 25, 27).

We previously showed that the majority of cytotoxic effector cells detected early after FV infection were NK rather than

* Corresponding author. Mailing address: Department of Immunology, Kinki University School of Medicine, 377-2 Ohno-Higashi, Osaka-Sayama, Osaka 589-8511, Japan. Phone and fax: 81-72-367-7660. E-mail: masaaki@med.kindai.ac.jp.

§ T. Ogawa and S. Tsuji-Kawahara contributed equally to this study.

† Present address: National Cerebral and Cardiovascular Center, Suita, Osaka, Japan.

‡ Department of Basic Medical Sciences, Kinki University Faculty of Medicine, Osaka-Sayama, Osaka, Japan.

▽ Published ahead of print on 16 March 2011.

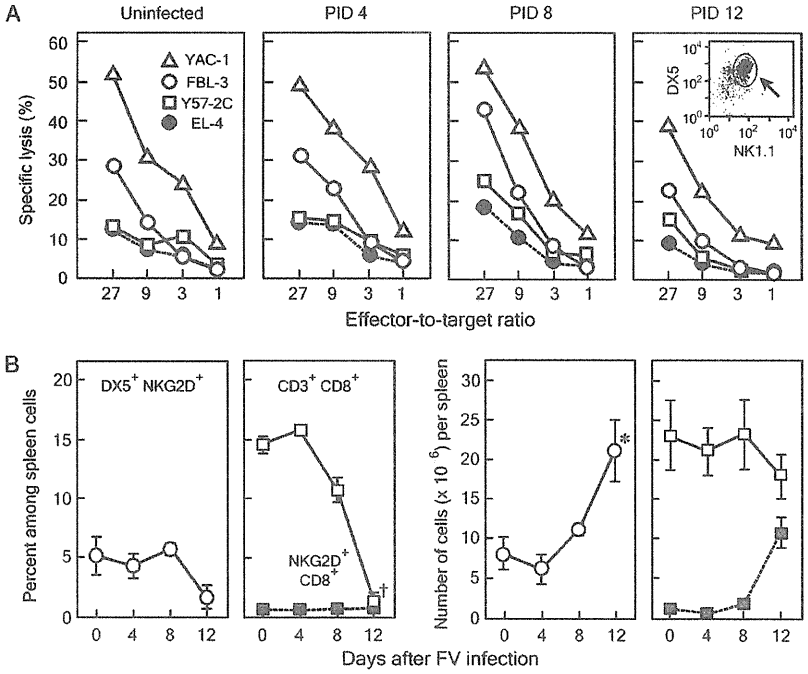


FIG. 1. Changes in NK cell activities and numbers in $CB6F_1$ mice after FV infection. (A) Killing activities of NK cells purified from $CB6F_1$ mice at various time points after FV infection on target cells of different origin. $CB6F_1$ mice were inoculated with 150 SFFU of LDV-free FV. $CD4^-$, $CD8^-$, $B220^-$, and $DX5^+$ NK cells were purified from the spleens, confirmed to be 85 to 95% positive for DX5 and 76 to 86% positive for both DX5 and NK-1.1 (arrow in the inset), and used as effector cells without an *in vitro* stimulation as described previously (16). Specific lysis of 4 different lines of target cells at each indicated effector-to-target ratio was measured by $^{51}Cr$ release assays (16, 45). Each data point here represents a mean calculated from triplicate wells with the SEM being <10% of the average throughout the present study. Experiments were repeated 3 times with essentially the same results. (B) Percentages and absolute numbers of NK and $CD8^+$ T cells expressing NKG2D at various time points after FV infection. $CB6F_1$ mice were inoculated with FV, and spleen cells were analyzed by multicolor flow cytometry. Absolute numbers of each cell population were calculated by (total number of nucleated spleen cells × percentage of the population in question)/100. Each data point here represents mean ± SEM calculated from 4 animals. *, $P < 0.05$ in comparison with the corresponding values at PID 0 (prior to infection) by *t* test; †, $P < 0.005$.

$CD8^+$ T cells (16). Further, protective anti-FV immunity induced by a single immunization of susceptible mice with a synthetic peptide that harbored a T-helper (Th) cell epitope (26) was totally abrogated by the depletion of NK cells, without affecting the numbers and proliferative and killing functions of $CD4^+$ and $CD8^+$ T cells (16). On the other hand, mice lacking $CD8^+$ T cells were nevertheless protected against FV infection by the above immunization with the single-epitope peptide (19). Our recent study (45) has revealed rapidly induced terminal exhaustion of $CD8^+$ effector cells in FV-infected animals; thus, although activated, FV-specific $CD8^+$ T cells become unable to exert cytotoxic effector functions upon cognate binding to infected target cells by as early as 14 days after infection. These results collectively indicate that NK cells, instead of $CD8^+$ T cells, may play essential roles in controlling the proliferation of erythroid progenitor cells in acute FV infection. In fact, enhanced NK cell activities were associated with delayed development of FV-induced leukemia in mice overexpressing vascular endothelial growth factor A (VEGF-A) (4). Here we utilized the above FV model to elucidate how retrovirus-infected cells are recognized by NK cells.

## MATERIALS AND METHODS

**Mice and virus.** C57BL/6 (B6; *Fv2*$^r$ *H2*$^b$) and (BALB/c × C57BL/6)$F_1$ ($CB6F_1$; *Fv2*$^{s/r}$ *H2*$^{d/b}$) mice were purchased from Japan SLC, Inc. (Hamamatsu, Japan). Breeding pairs of B6(Cg)-*Tnfrsf13c*$^{tm1Mass}$/J (B6-*BAFF-R*$^{-/-}$) mice homozygously carrying a targeted disruption of the receptor for B-cell activating factor belonging to the tumor necrosis factor family (*BAFF-R*) gene (37) were purchased from The Jackson Laboratory (Bar Harbor, ME). The apolipoprotein B mRNA editing enzyme catalytic polypeptide 3 (APOBEC3)-deficient mice on a B6 background (B6-*APOBEC3*$^{-/-}$) have been described previously (46, 47). Mice 8 to 12 weeks in age at the time of FV infection were used throughout the present study. The stocks of B-tropic FV without contamination of lactate dehydrogenase-elevating virus (LDV) and the infectious molecular clone of F-MuLV, FB-29, have been described previously (27, 45–47). Mice were inoculated with an indicated dose of FV or F-MuLV by intravenous injection into the tail vein. All animal experiments described here have been approved by the Animal Experiment Committee of Kinki University and performed according to the relevant laws and regulations of the Japanese government.

**Purification of NK cells and cytotoxicity assays.** Purification of NK cells was performed by using antibody (Ab)-conjugated micromagnetic beads as described previously (16), except that an automated magnetic cell sorting separator (autoMACS; Miltenyi Biotech GmbH, Bergisch Gladbach, Germany) was used in the present study. In brief, nucleated spleen cells in phosphate-buffered balanced salt solution (PBBS) were first mixed with a mixture of anti-mouse CD4, anti-mouse CD8, and anti-mouse B220 Ab-conjugated microbeads solution, and $CD4^+$, $CD8^+$, and $B220^+$ cells were depleted by using the Depletes program. The resultant $CD4^-$, $CD8^-$, and $B220^-$ cells were then mixed with anti-DX5 Ab-conjugated microbeads, and positive selection was performed by using the Posselds program. The resultant $CD4^-$, $CD8^-$, $B220^-$, and $DX5^+$ cells were confirmed to be 85 to 95% positive for DX5 (Fig. 1A, inset) and were used as effector cells without any *in vitro* stimulation throughout the present study. The target cells used were as follows: an F-MuLV-induced leukemia cell line, FBL-3, established from a B6 mouse; a line of FV-induced leukemia cells, Y57-2C, established from a (C57BL/10 × A.BY)$F_1$ (*H2*$^{b/b}$) mouse; a chemically induced

T-cell lymphoma line, EL-4, established from a B6 mouse; and an A/Sn mouse-derived Moloney murine leukemia virus (M-MuLV)-induced lymphoma line, YAC-1 ($H2^a$). Y57-2C cells were originally provided by Bruce Chesebro, Laboratory of Persistent Viral Diseases, NIH, NIAID, Rocky Mountain Laboratories, Hamilton, MT, and FBL-3, EL-4, and YAC-1 cells were provided by Kagemasa Kuribayashi, Mie University School of Medicine, Tsu, Japan. Cytotoxicity assays were performed by using $^{51}$Cr-labeled target cells as described elsewhere (16, 45).

For the possible blocking of NK-mediated killing, low-endotoxin and azide-free functional-grade anti-mouse NKG2D Ab (clone CX5, rat IgG1 [29], and clone C7, Armenian hamster IgG [13]) were purchased from eBioscience (San Diego, CA) and added to the assay cultures at 30 μg/ml according to a previously described procedure (13). Control IgG1 purified from unimmunized rat sera and monoclonal Ab A19-3 (Armenian hamster IgG) specific for trinitrophenyl hapten were purchased from eBioscience and BD Biosciences PharMingen (San Diego, CA), respectively.

**Flow cytometry.** Flow cytometric analyses were performed as described elsewhere (44–47). Abs used were the following: fluorescein isothiocyanate (FITC)-conjugated anti-mouse CD8α and phycoerythrin (PE)-conjugated anti-mouse NKG2D (clone CX5) (eBioscience); FITC-conjugated anti-NK1.1, biotin-conjugated anti-mouse Pan-NK (DX5), biotin-conjugated anti-mouse Qa-$1^b$, and allophycocyanin (APC)-conjugated anti-mouse TER-119 (BD Biosciences PharMingen); and PE-conjugated anti-mouse Pan–RAE-1 (R&D Systems, Inc., Minneapolis, MN). B6 mice express the alloantigen NK-1.1, and DX5 recognizes CD49b (2). TER-119 reacts with a molecule associated with glycophorin A (20) and marks late erythroblasts as well as mature red cells (50). Monoclonal Ab 720 reactive with F-MuLV gp70, but not with any other mouse retrovirus (36), was purified and conjugated with biotin as described previously (45–47). PE-conjugated (BD Biosciences PharMingen) and FITC-conjugated (DakoCytomation, Glostrup, Denmark) streptavidin were used for staining with the biotin-conjugated antibodies. All staining reactions were performed in the presence of 0.25 μg/$10^6$ cells of anti-mouse CD16/CD32 (BD Biosciences PharMingen). Cells were also incubated with the appropriate isotype-matched control Ab to draw demarcation lines that separate cells positively stained from those not stained. Multicolor flow cytometric analyses were performed with a Becton-Dickinson FACSCalibur and CellQuest software (BD Biosciences, Franklin Lakes, NJ).

**Depletion of NK cells and blocking of NKG2D–RAE-1 interactions *in vivo*.** Rabbit antiserum specific for mouse asialo ganglio-*N*-tetraosylceramide (asialo-GM1) and control normal rabbit serum were purchased from Wako Pure Chemicals (Osaka, Japan), and the IgG fraction was concentrated by precipitation with 45% (final) ammonium sulfate. Mice were injected intravenously with 60 μg/dose of the anti-asialoGM1 Ab at 1 day prior to FV inoculation and 2, 5, 8, and 11 days after the virus infection as performed previously (16). For *in vivo* blocking of NKG2D, 100 μg/dose anti-NKG2D Ab (CX5) or control rat IgG was administered 2 days prior to, the day of, and 2 days after FV inoculation. The lack of a detectable level of NKG2D on $DX5^+$ NK cells was confirmed 5 days after infection by flow cytometry essentially as described previously (45). Monoclonal anti-mouse RAE-1 Ab that blocks the binding of mouse NKG2D to β and δ isoforms of mouse RAE-1 (clone 199205, rat IgG2b) (51) was purchased from R&D Systems, Inc., and 100 μg/dose of this Ab or the above control rat IgG was administered the day of and 2 days after FV inoculation.

FV-induced disease development was monitored by following the survival of each representative group of infected mice for 60 days and by measuring spleen weights at 13 days after infection as described previously (16, 19). Infectious center assays were performed as described previously (19, 26). Three-fold dilutions of nucleated spleen cells between 30 and $3 \times 10^6$/well were prepared from each animal and were added in triplicate into a well of 24-well tissue culture plates that had been seeded with $1 \times 10^4$ *Mus dunni* cells on the previous day. Spots of F-MuLV gp70-expressing *Mus dunni* cells in each well were counted under a magnifier after 2 days of coculturing followed by fixation and immunoenzymatic staining with monoclonal Ab 720 (36). The numbers of spleen infectious centers were calculated as averages of triplicate samples which gave close to but less than 150 spots of the infected indicator cells per well. As up to $3 \times 10^6$ nucleated spleen cells can be seeded and up to 150 spots of infected *Mus dunni* cells can be distinguished per well, the results shown in the present study represent absolute numbers of infectious centers among $10^5$ nucleated spleen cells.

**Quantitative real-time PCR assays.** For the induction of NK receptor ligands, the indicated leukemia and lymphoma cells maintained in an exponential growth phase were reseeded at $2.5 \times 10^6$ cells/5 ml/well in 6-well tissue culture plates with 5 U/ml (final) of recombinant mouse gamma interferon (IFN-γ) (BD Biosciences PharMingen). After the indicated hours of incubation, cells were harvested and total cellular RNA was extracted by using the TRIzol solution (Invitrogen Japan, K. K., Tokyo, Japan). Poly-$A^+$ RNA was purified from total RNA for each sample by the use of the MicroFast Track 2.0 system (Invitrogen).

Quantitative real-time PCRs were performed as described previously (46, 47). The sequence-specific primers and probes used are as follows: *Raet1* forward, CGCCATCATTTTATGATTCAGAAG, reverse, TGGTCAAGTTGCACCTA AGAGAGT, and probe, 6-carboxyfluorescein (FAM)-TACTGAGCTATGGAT ACACCAACGGGCTZ-6-carboxytetramethylrhodamine (TAMRA); *Qa-1$^b$* forward, AGATCTCTAAGCACAAGTCAGAGGC, reverse, TCATTTCCCAGC CGTAGGTATC, and probe, FAM-TGAGGCCCACCAACAGAGGGCATZ-TAMRA; and F-MuLV *env* forward, GCTGCGAGACAACCGGTAGA, reverse, GCATACCTGAACAGCCTGGTTA, and probe, FAM-TTCTTGGGA CTACATCACAGTZ-TAMRA. The above primer/probe set used for the detection of the *Raet1* messages reacts with all known isoforms (α-ε) of mouse *Raet1*. Specificities of the probes were confirmed by cloning and sequencing the amplified cDNA fragments as described previously (46). TaqMan rodent *GAPDH* control (Applied Biosystems, Foster City, CA) was added to each reaction mixture as a normalizer. The levels of expression of each gene tested were expressed by the threshold cycle ($2^{-\Delta CT}$), where an average value and SEM were calculated for each sample.

**Statistical analyses.** Two-way analysis of variance (ANOVA) with Bonferroni *post hoc* tests and Mantel-Cox tests of survival curves were performed by using Prism software (GraphPad Software, Inc., San Diego, CA). Average values were compared by Student's or Welch's *t* test, depending on whether the variances of the compared samples were estimated to be equal or not, and Bonferroni's correction was applied for multiple comparisons when required. Paired *t* tests were performed when two parameters within a single experimental group were compared.

## RESULTS

**Changes in NK cell activities upon FV infection of susceptible mice.** Mice possessing at least a single dominant $Fv2^s$ allele develop polycythemia and splenomegaly early after FV inoculation. $CB6F_1$ mice are highly susceptible to FV and develop massive splenomegaly within 2 weeks after infection, and all die within 60 days upon inoculation, with as low as 15 spleen focus-forming units (SFFU) of FV (16, 19, 26, 27). NK cell activities were previously demonstrated with the spleens of $CB6F_1$ mice at 7 to 11 days after FV infection (16); however, the *in vivo*-passaged FV stocks used in the above and other experiments performed prior to 2007 had been contaminated unintentionally with LDV, which is known to activate NK cells soon after inoculation (27). It is possible, therefore, that the previously detected NK cell activities were evoked by LDV, rather than by FV infection. Thus, we first tested the killing activities exerted by NK cells purified from $CB6F_1$ mice at various time points after infection with LDV-free FV.

High-level killing activities were detectable against YAC-1 target cells even before FV inoculation of $CB6F_1$ mice. Killing activities against F-MuLV-induced FBL-3 tumor cells were also detected prior to FV infection, increased following FV infection, and peaked at postinoculation day (PID) 8 (Fig. 1A). Both activities, however, decreased at PID 12. The above kinetics were essentially not different from those observed by inoculating the same strain of mice with an LDV-contaminated stock of FV (data not shown). Thus, FV infection without LDV contamination enhanced constitutively detectable NK-mediated killing activities against F-MuLV-induced FBL-3 leukemia cells in $CB6F_1$ mice.

**Different levels of NK-receptor ligand expression in correlation with susceptibility to NK-mediated lysis among retrovirus-induced leukemia cell lines.** In the previously (16) and the above-described (Fig. 1A) experiments, the FV-induced leukemia line Y57-2C cells were almost as resistant to NK-mediated killing as EL-4 lymphoma cells were, while F-MuLV-

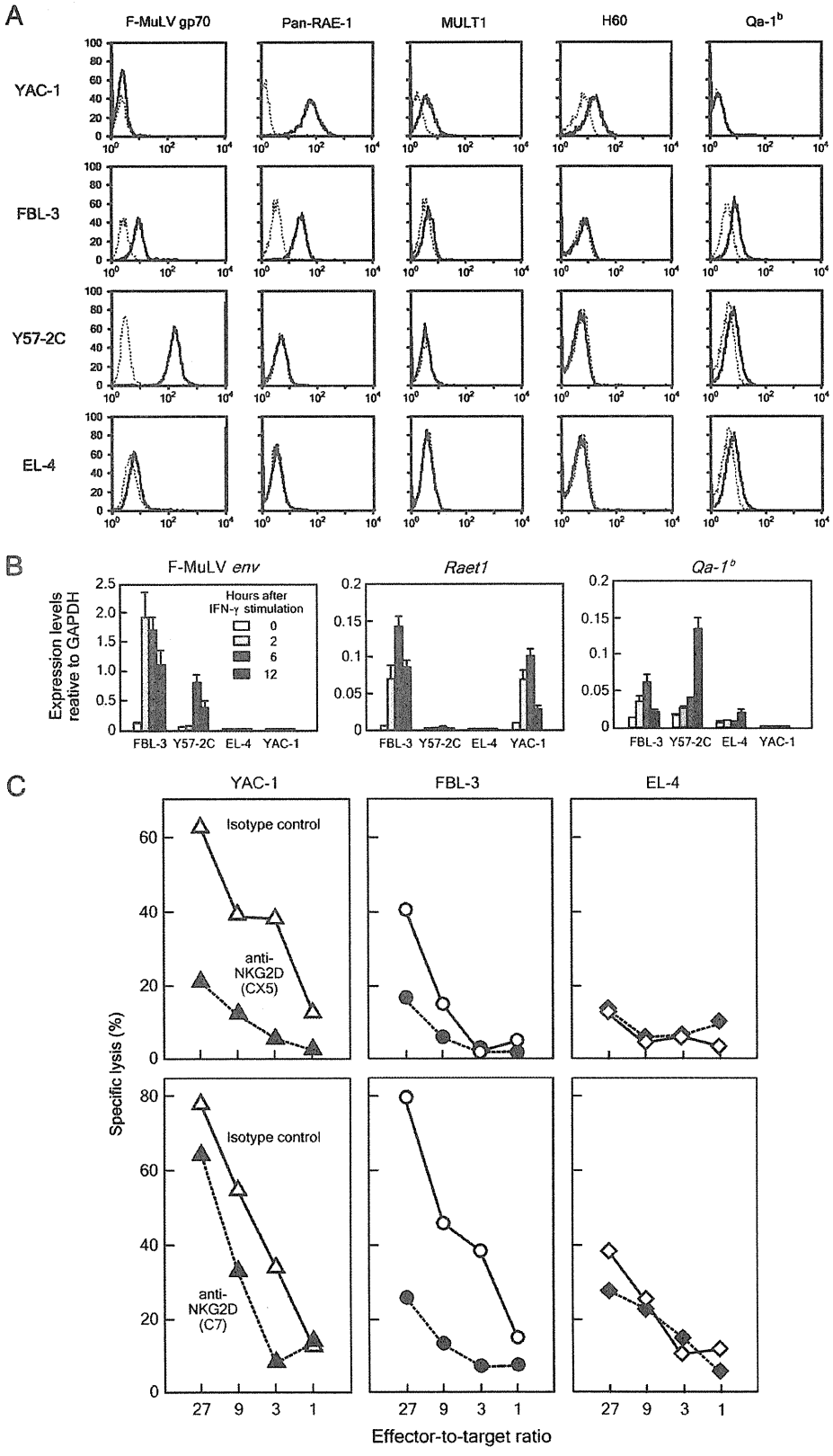
A
F-MuLV gp70
Pan-RAE-1
MULT1
H60
Qa-1b
YAC-1
FBL-3
Y57-2C
EL-4
B
F-MuLV env
Raet1
Qa-1b
Expression levels reative to GAPDH
Hours after IFN-γ stimulation
0
2
6
12
FBL-3 Y57-2C EL-4 YAC-1
C
YAC-1
FBL-3
EL-4
Isotype control
anti-NKG2D (CX5)
anti-NKG2D (C7)
Specific lysis (%)
Effector-to-target ratio
27 9 3 1

induced FBL-3 leukemia cells were killed almost as efficiently as positive control YAC-1 cells by NK cells purified from FV-infected mice at around PID 8. The above different susceptibilities to NK killing between FBL-3 and Y57-2C cells were observed regardless of the days after FV infection and whether FV stocks used were contaminated with LDV (16) or not (Fig. 1A), indicating that the differences in NK susceptibility were determined mainly by the intrinsic nature of each target cell line, not by the possibly different activation statuses or subsets of the effector cells.

We therefore analyzed the expression of various ligand molecules that are recognized by inhibitory and activating NK receptors: RAE-1 family proteins, the product of the murine ULBP-like transcript-1 (MULT1) gene, and H60 molecules, all of which interact with the major activating NK receptor NKG2D; and MHC class Ib Qa-1 molecules, encoded by the *H2-T23* locus, that are recognized by both inhibitory NKG2A/CD94 and activating NKG2C/CD94 and NKG2E/CD94 receptor complexes (30, 49). As mouse genes encoding RAE-1 molecules (*Raet1*) are polymorphic and B6 mice express the RAE-1δ and -1ε isoforms while other strains, such as BALB/c and NOD, express RAE-1α, -1β, and -1γ (22, 30), we utilized the anti-Pan–RAE-1 Ab that reacted with all 5 isoforms.

NK-susceptible YAC-1 and FBL-3 cells both expressed RAE-1 molecules on their surfaces at high levels, while NK-resistant Y57-2C and EL-4 cells lacked the expression of RAE-1 (Fig. 2A). In addition, the most highly NK-susceptible YAC-1 cells expressed other NKG2D ligands, MULT1 and H60, while only low-level expression of MULT1, but not H60, was detectable on FBL-3 cells. As YAC-1 cells were established from an A/Sn mouse and FBL-3 from a B6 mouse, the above results are consistent with the fact that B6 mice lack the expression of H60 (22). All three cell lines (FBL-3, Y57-2C, and EL-4) established from an $H2^b$-possessing strain of mice constitutively expressed the product of the $H2\text{-}T23^d$ ($Qa\text{-}1^b$) allele, while YAC-1 cells homozygous for the $H2^a$ haplotype lacked the expression of $Qa\text{-}1^b$.

As the expression of RAE-1 family molecules, as well as Qa-1, is inducible and *Raet1* genes are induced by IFN-γ (8), which plays a crucial role in immune protection against FV infection (7, 31, 32, 42), we also examined the possible changes in the expression levels of genes encoding these ligands after IFN-γ stimulation. As predicted, only the F-MuLV-infected leukemia cells, FBL-3 and Y57-2C, expressed transcripts from the viral *env* gene, and their expression levels were markedly enhanced after stimulation with IFN-γ (Fig. 2B). Stimulation of the two NK-susceptible lines of cells with IFN-γ resulted in a rapid rise in the levels of the *Raet1* messages; however, no significant expression of the *Raet1* messages was detected in Y57-2C and EL-4 cells even after IFN-γ stimulation, confirming the lack of expression of RAE-1 in these NK-resistant cell lines. The expression levels of the $Qa\text{-}1^b$ allele in FBL-3 and Y57-2C cells increased after IFN-γ stimulation, as has been reported previously (14), but YAC-1 cells again lacked the expression of the $Qa\text{-}1^b$ message.

**NK killing of FBL-3 target cells was mediated via the NKG2D receptor.** To directly assess the above-indicated putative correlation between the expression of NKG2D ligand RAE-1 molecules and susceptibility to killing by NK cells, two monoclonal Abs that block the interaction between NKG2D and its ligands (13, 29) were added separately to the wells of killing assays. The lysis of FBL-3 target cells by NK cells purified from FV-infected $CB6F_1$ mice was abrogated to the levels of that against NK-resistant EL-4 cells by the addition of either of the blocking Abs in repeated experiments (Fig. 2C). The killing of YAC-1 cells was also blocked, at least partially, by the anti-NKG2D Ab, but significant lytic activities were detectable at higher effector-to-target ratios even in the presence of the anti-NKG2D Ab, consistent with the previous finding that YAC-1 cells are killed by NK cells through both NKG2D-dependent and -independent signaling pathways (17). Thus, the results shown in Fig. 1A and 2 collectively indicate that NK cells purified from FV-infected $CB6F_1$ mice recognize F-MuLV-induced FBL-3 target cells mainly through the NKG2D–RAE-1 interactions.

**Expansion of $NKG2D^+$ cells and induction of NKG2D ligand expression on infected erythroid progenitor cells in the spleens of FV-inoculated mice.** We next examined the possible changes in percentages and absolute numbers of $NKG2D^+$ cells in the spleens of FV-infected mice. Since NKG2D is known to be expressed by NK as well as a population of $CD8^+$ effector cells (17), the percentages of $NKG2D^+$ cells among $CD8^+$ T cells were also analyzed. The percentages of $CD3^+$ $CD8^+$ T cells in the spleen significantly decreased by 12 days after FV infection (Fig. 1B); however, as total numbers of spleen cells increased following FV infection, absolute numbers of $CD3^+$ $CD8^+$ T cells did not change significantly during the 12-day period of acute FV infection. On the other hand, absolute numbers of $DX5^+$ $NKG2D^+$ cells started to increase by PID 8 and became significantly higher than those prior to infection at PID 12. Thus, NK cells expanded upon FV infection. Interestingly, significant percentages and numbers of

FIG. 2. Correlation between the expression of different NK receptor ligands and susceptibility to NK killing of 4 different cell lines. (A) Cell surface expression of NK receptor ligands and F-MuLV gp70 on the 4 lines of cells were analyzed by flow cytometry. Shown here are histograms, with each horizontal axis showing fluorescence intensity observed with the indicated Ab. Dotted lines indicate reactivity of isotype control Ab. (B) Real-time PCR quantification of the expression levels of NK receptor ligand genes. Indicated cells were cultured in the presence of 5 U/ml IFN-γ, and total RNA was extracted at the indicated time points after the stimulation. Specificity of each of the primer sets was confirmed by separate plasmid cloning and sequencing of the amplified DNA fragments. The levels of expression of each tested gene are shown by $2^{-\Delta CT}$ values by using *GAPDH* as a normalizer. Results shown here are mean ± SEM calculated with data from 2 or 4 reaction wells for each sample dilution. The experiments were repeated 4 times with essentially the same results. (C) Blocking of NK-mediated killing by the anti-NKG2D Ab. Effector NK cells were purified from $CB6F_1$ mice at 8 days after inoculation with FV and confirmed to be >85% positive for both NK-1.1 and DX5. Blocking CX5 (top) or C7 (bottom) Ab (filled symbols) and each corresponding isotype control Ab (open symbols) were added at a final concentration of 30 μl/ml according to the previous report (13). The optimality of the above working concentration was confirmed in preliminary experiments. Each data point here represents a mean calculated from quadruplicated wells, with the SEM being <10% of the average throughout the present study. The blocking experiments were repeated 4 times with each Ab and showed essentially the same results.

$DX5^+$ $NKG2D^+$ NK cells were present in the spleens of $CB6F_1$ mice even before FV infection, consistent with the high baseline NK activities detectable in $CB6F_1$ mice (Fig. 1A). The proportion of $NKG2D^+$ cells among $CD8^+$ T cells remained low until PID 8, but the absolute numbers of $NKG2D^+$ $CD8^+$ cells abruptly increased by PID 12.

As to the expression of NKG2D ligands on FV-infected cells *in vivo*, flow cytometric analyses revealed increased expression of RAE-1 and MULT1, but not H60, on the surfaces of $gp70^+$ and TER-$119^+$ erythroid progenitor cells in the spleens of FV-infected $CB6F_1$ mice (Fig. 3A). As shown in Fig. 3A, $gp70^+$ cells were only slightly increased in the spleen until PID 8. Nevertheless, >1/5 of the $gp70^+$ cells expressed RAE-1 above the level of the demarcation line, while a large majority of $gp70^-$ cells were also negative for RAE-1. By PID 12, $gp70^+$ populations increased drastically, and a significant proportion of them expressed RAE-1 above the level of the demarcation line. At the same time point, three distinctive populations of $gp70^+$ cells with undetectable levels of TER-119 expression (TER-$119^-$ $gp70^+$ cells), low levels of TER-119 and high gp70 expression (TER-$119^{Lo}$ $gp70^{Hi}$ cells, purple dots, Fig. 3A), and TER-$119^{Hi}$ $gp70^+$ erythroblasts (red dots, Fig. 3A) appeared in the spleen. Based on a previous report (50), these three populations of $gp70^+$ cells most likely represent distinctive stages of erythroid cell differentiation from FV-infected progenitor cells, including primitive erythroid progenitor cells and proerythroblasts (TER-$119^-$), proerythroblasts and early basophilic erythroblasts (TER-$119^{Lo}$), and maturing benzidine-positive erythroblasts (TER-$119^{Hi}$). Importantly, the TER-$119^{Lo}$ population that showed higher levels of gp70 expression than the two other populations also showed higher levels of RAE-1 and MULT1 expression on their surfaces, but their levels of H60 expression were below the detection limit (Fig. 3A).

When mean fluorescence intensities were compared between different populations of spleen cells, the average levels of RAE-1 expression on the surfaces of $gp70^+$ cells were significantly higher than those on $gp70^-$ cells in $CB6F_1$ mice at all time points tested (Fig. 4). Further, TER-$119^{Lo}$ proerythroblasts and early basophilic erythroblasts expressed significantly higher levels of RAE-1 on their surfaces than TER-$119^-$ cells at PID 12, indicating that FV-infected erythroid cells can become susceptible to NK killing due to RAE-1 upregulation.

**Decreased MHC class I and class Ib antigen expression on terminally differentiating erythroid cells.** The target-killing activities of NK cells are regulated not only by the above positive signals but also by negative signals generated by receptors binding to MHC molecules, and the MHC class Ib $Qa\text{-}1^b$ molecule is a strong inhibitor of NK activities in mice (49). Thus, FV-infected erythroid cells might also become susceptible to NK killing due to their possibly reduced expression of class I and/or class Ib molecules. As shown in Fig. 3B, the TER-$119^-$ population of spleen cells retained high levels of MHC class I $K^b$ and lower levels of $D^b$ molecules, as well as class Ib $Qa\text{-}1^b$, on their surfaces until PID 12; however, decreased expression of $Qa\text{-}1^b$, as well as $K^b$ and $D^b$, was discernible in a small population of TER-$119^+$ erythroid cells at PID 4 and 8 (data not shown). At PID 12, TER-$119^{Hi}$ terminally differentiating erythroid cells (Fig. 3B, pink dots) showed markedly diminished expression of the class I molecules, and $Qa\text{-}1^b$ expression on the majority of TER-$119^{Hi}$ cells became barely detectable. It is notable, however, that the TER-$119^{Lo}$ cells that showed increased expression of RAE-1 (Fig. 3A) retained unchanged levels of class I and $Qa\text{-}1^b$ expression, and the lack of $Qa\text{-}1^b$ expression was observed only with the TER-$119^{Hi}$ population. As levels of RAE-1 and MULT1 expression, as well as those of viral gp70, on the surfaces of TER-$119^{Hi}$ cells were also reduced in comparison with those on TER-$119^{Lo}$ cells at PID 12 (Fig. 3A), these observations may reflect the global downregulation of gene expression in terminally differentiating erythroid cells (33, 40). Thus, $gp70^{Hi}$ TER-$119^{Lo}$ erythroblasts that are massively increased in the spleen by PID 12 express higher levels of RAE-1 and MULT1 but retain the expression of $Qa\text{-}1^b$.

***In vivo* role of NKG2D–RAE-1 interactions in controlling early expansion of FV-infected cells and the development of virus-induced pathologies.** Although the above experiments have shown significant expansion of $NKG2D^+$ NK cells and increased expression of RAE-1 proteins on infected erythroid cells upon FV inoculation, the sufficiency of the levels of RAE-1 expression induced in TER-$119^{Lo}$ erythroid cells to evoke NK-mediated killing in the presence of $Qa\text{-}1^b$ can be questioned. In this regard, the Ab-mediated depletion of NK cells from mice immunized with a single-epitope peptide vaccine totally abrogated the protective efficacy of Th cell priming, and NK-depleted mice died as rapidly as unimmunized control mice after FV infection in the previous experiments (16). However, the possible physiological role of NK cells in regulating the early proliferation of FV-infected erythroid cells in unimmunized mice of a susceptible strain has not been analyzed. To address this, we administered anti-asialoGM1 Ab to unimmunized $CB6F_1$ mice and reduced the percentages of $DX5^+$ NK-$1.1^+$ NK cells in the spleen to <1.2 through PID 4 to 12. In the above NK-depleted mice, the number of FV infectious centers in the spleen drastically increased at as early as PID 6 (Fig. 5A), indicating that NK cells are actually restricting early expansion of FV-infected cells in the spleen. The percentages of $gp70^+$ cells in the spleen at 6 days after FV infection also increased significantly in the NK-depleted mice and became 3 times higher than those in the control mice infected without NK depletion (Fig. 5B). As $CB6F_1$ mice are highly susceptible to FV-induced disease development, the percentages of $gp70^+$ cells in the spleen increased toward PID 12 in both groups; however, the proportions of $gp70^+$ cells further increased in the absence of asialoGM$1^+$ cells in comparison with those in the control animals given unimmunized sera. Importantly, NK cell depletion also affected the survival of FV-infected mice: when inoculated with a slightly reduced dose of 50 SFFU, highly susceptible $CB6F_1$ mice still developed the fatal disease and most died by 60 days after FV infection, while NK-depleted $CB6F_1$ mice died significantly more rapidly, with an average survival period that was 9 days shorter than that of the control mice (Fig. 5C). These results indicate that NK cells are not only involved in confining the early expansion of FV-infected erythroid cells, but are contributing to natural resistance to FV-induced disease development in unimmunized animals.

Although the administration of anti-asialoGM1 Ab did not affect $CD4^+$ and $CD8^+$ T-cell numbers and their functionalities in the previous experiments (16), it is possible that FV-reactive T cells, along with NK cells, might have been affected

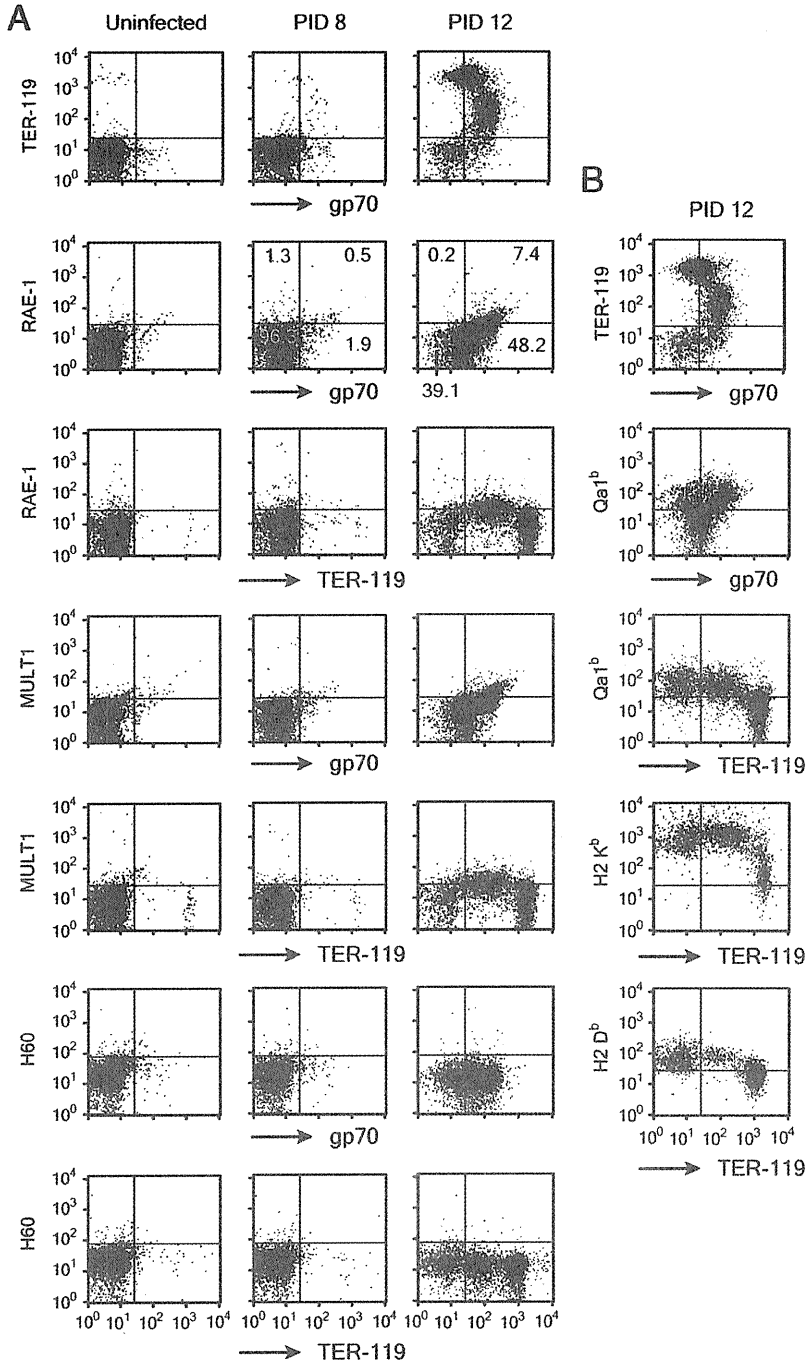


FIG. 3. Representative dot plots showing the expression of NK receptor ligand proteins (A) and MHC class I and class Ib molecules (B) on the surfaces of spleen cells in FV-infected CB6F$_1$ mice. CB6F$_1$ mice were inoculated with 150 SFFU FV, and at least 4 mice were killed at PID 4, 8, and 12 to remove the spleen. Multicolor flow cytometric analyses were performed with each indicated Ab. Uninfected mice were similarly analyzed as controls. Mature erythrocytes and dead cells were excluded by setting a polygonal gate in the dot plots showing intensities of forward scatter and the fluorescence for 7-aminoactinomycin D. Demarcation lines were set based on the fluorescence levels observed by incubating the cells with isotype control Ab. Data on PID 4 are omitted from this figure, as they are essentially similar to those on PID 8, except that gp70$^+$ populations are much smaller. In the middle and right panels of the second row of dot plots in panel A, the number in each quadrant represents the percentage of cells that expressed the indicated markers above or below the level of the corresponding demarcation line. Patterns observed with all 4 mice at each time point were consistent with those shown here. In panel A, purple dots, TER-119$^{Lo}$ gp70$^{Hi}$ cells; red dots, TER-119$^{Hi}$ gp70$^+$ erythroblasts. In panel B, red dots, TER-119$^{Lo}$ gp70$^{Hi}$ cells; pink dots, TER-119$^{Hi}$ gp70$^+$ erythroblasts.

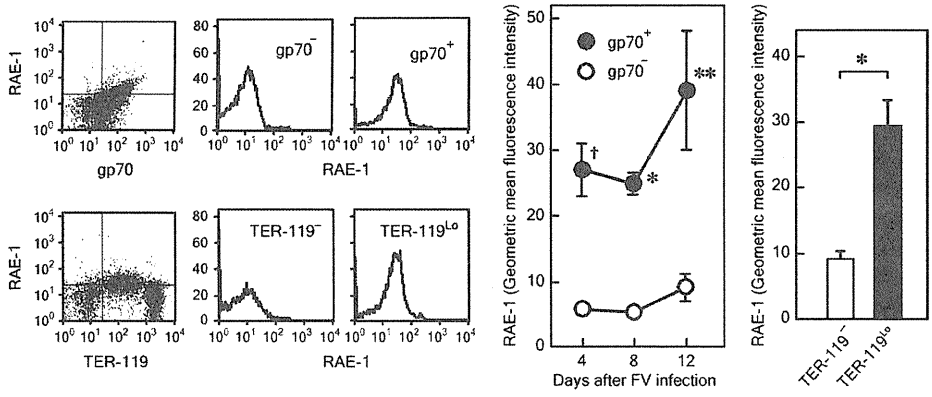


FIG. 4. Different levels of RAE-1 expression between viral gp70-positive and -negative spleen cells in mice infected with FV. $CB6F_1$ mice were inoculated with 150 SFFU of LDV-free FV, and multicolor flow cytometric analyses were performed on nucleated cells as described for Fig. 3. Representative dot plots and histograms on the left show different levels of RAE-1 expression on pairs of $gp70^-$ and $gp70^+$ or $TER\text{-}119^-$ and $TER\text{-}119^{Lo}$ populations at PID 12. $TER\text{-}119^-$ and $TER\text{-}119^{Lo}$ populations are those shown with black and purple dots, respectively, in Fig. 3A. Changes in averages of geometric mean fluorescence intensity (GMFI) for RAE-1 among $gp70^-$ and $gp70^+$ cells after FV infection are shown in the middle panel. GMFI were calculated by using the region statistics function of the CellQuest software. Each datum shown here is the mean ± SEM. calculated with GMFI data obtained from 4 mice. Differences between $gp70^+$ and $gp70^-$ populations were examined by two-way ANOVA with Bonferroni *post hoc* tests: *, $P < 0.05$; †, $P < 0.01$; **, $P < 0.001$. The right panel shows averages of GMFI for RAE-1 compared between the $TER\text{-}119^-$ and $TER\text{-}119^{Lo}$ populations at PID 12. Each bar shows mean ± SEM calculated with GMFI data obtained from 4 or 5 mice. *, $P < 0.02$, by paired $t$ test.

by the Ab injections in the above depletion experiments, as activated T cells are known to express asialoGM1 in some viral infections (41). To further demonstrate the direct involvement of the RAE-1 ligand and NKG2D receptor in confining the early expansion of FV-infected cells, blocking Abs were administered to infected $CB6F_1$ mice. The numbers of FV-producing cells in the spleen significantly increased in the animals that were given either NKG2D- or RAE-1-blocking Ab in comparison with those in the control mice (Fig. 5A and D). Further, in the presence of the RAE-1-blocking Ab, FV-infected $CB6F_1$ mice showed significantly larger spleen sizes than control mice (Fig. 5E), confirming that FV-infected erythroid progenitor cells are recognized and their expansion is regulated through NKG2D–RAE-1 interactions *in vivo*. As the effects of the NKG2D or RAE-1 blockade were observed at as early as PID 6, prior to the expansion of $NKG2D^+$ $CD8^+$ T cells (Fig. 1B), it is most likely that mainly $NKG2D^+$ NK cells were responsible for the above early confinement of FV-induced erythroid cell proliferation.

**Increased expression of RAE-1 depends on retroviral replication rather than on erythroid cell proliferation.** As the FV complex induces massive proliferation and terminal differentiation of erythroid progenitor cells in mice possessing the $Fv2^s$ allele, the above-described increase in RAE-1 expression on $TER\text{-}119^{Lo}$ cells may depend on the specific differentiation stage (proerythroblasts and early basophilic erythroblasts) or activated status of red cell precursors, rather than on FV infection. To examine this, we first induced an increased erythropoiesis by administering phenylhydrazine (PHZ) instead of FV infection. After administration of PHZ, both the $TER\text{-}119^{Lo}$ and $TER\text{-}119^{Hi}$ populations became discernible in the spleens of $CB6F_1$ mice; however, neither population in PHZ-treated mice showed increased expression of RAE-1, unlike the $gp70^+$ $TER\text{-}119^{Lo}$ population in FV-infected mice (Fig. 6A). Similar results were also obtained for MULT1. Thus, the increase in RAE-1 and MULT1 expression on the $TER\text{-}119^{Lo}$ population was likely caused by FV infection, not by induced erythropoiesis.

To further elucidate putative relationships between FV replication and RAE-1 expression on target cells of FV infection, mice deficient of either of the FV resistance factors APOBEC3 and BAFF-R, which show markedly enhanced FV replication and exaggerated pathology (46, 47), were examined. Mice of the $Fv2^{r/r}$ background were utilized so that the effects of FV replication on RAE-1 expression could be further separated from those of SFFV-induced erythroid cell proliferation. Both APOBEC3- and BAFF-R-deficient mice showed markedly increased numbers of gp70-expressing cells in the spleen in comparison with those in the wild-type (WT) animals (Fig. 6B). Importantly, RAE-1-positive cells increased in association with the increased numbers of $gp70^+$ cells in APOBEC3- and BAFF-R-deficient animals. In APOBEC3-deficient mice, most of the $gp70^+$ cells were $TER\text{-}119^+$ and $B220^-$, and these cells showed increased expression of RAE-1 proteins on their surfaces (Fig. 6B, arrows). In mice deficient of BAFF-R, even larger numbers of both $TER\text{-}119^+$ (Fig. 6B, orange dots) and $TER\text{-}119^-$ cells (Fig. 6B, red dots) were infected with FV, and these $gp70^+$ cells expressed higher levels of RAE-1 than $gp70^-$ cells. Interestingly, in FV-infected $BAFF\text{-}R^{-/-}$ mice a significant proportion of $B220^+$ B lymphocytes were also infected with FV, and they expressed higher levels of RAE-1 than uninfected B cells (Fig. 6B, blue dots).

As SFFV-induced growth potentiation of erythroid cells is limited in the above-described $Fv2^r$ B6-background mice and as $gp70^+$ B cells, as well as erythroid cells, expressed higher levels of RAE-1 proteins than $gp70^-$ cells, the above results suggested that the replication of F-MuLV alone in the absence of SFFV might induce increased RAE-1 expression on target cells. Thus, we next infected the same gene-targeted animals with an infectious molecular clone of F-MuLV. In APOBEC3-

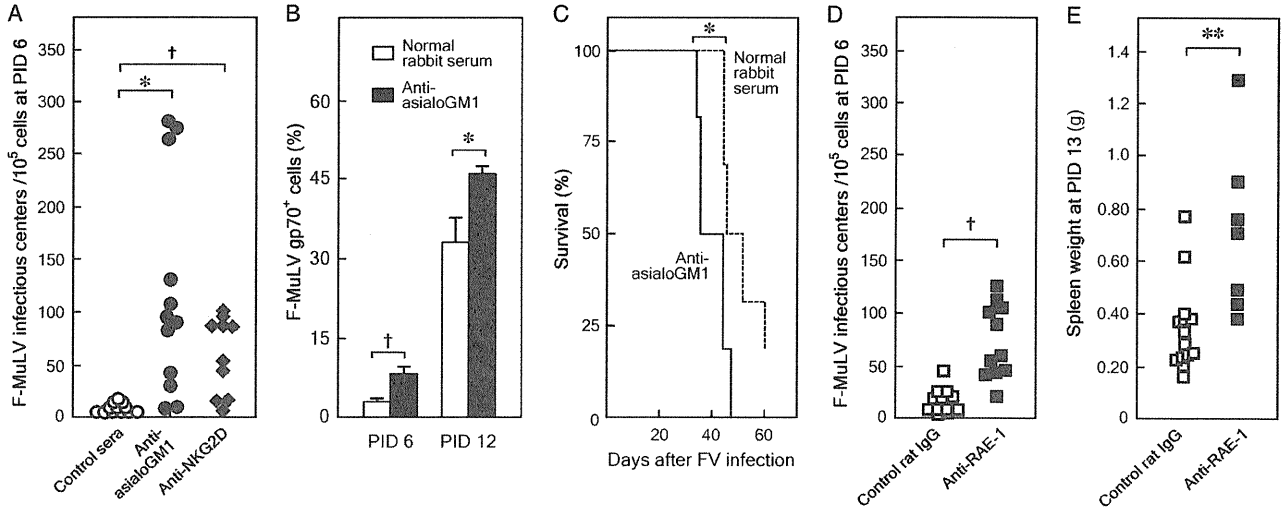


FIG. 5. Effects of the administration of anti-asialoGM1, anti-NKG2D, or anti-RAE-1 Ab on the expansion of virus-producing cells in the spleen and the development of FV-induced pathologies. (A) $CB6F_1$ mice were injected with either the anti-asialoGM1 or the blocking anti-NKG2D Ab and inoculated with 150 SFFU of FV. Control mice were injected with a mixture of normal rabbit and normal rat sera (control sera), and similarly infected. F-MuLV infectious centers in the spleen were enumerated by fluorescent focus assays as described previously (19, 44–47). Each symbol represents a datum from an individual mouse. As the anti-asialoGM1 and anti-NKG2D Ab-injected groups were compared with the common control group given the mixture of unimmunized sera, Bonferroni's correction was performed for multiple comparisons: *, $P = 0.0028 < \alpha(0.05) = 0.0253$; †, $P < 0.0005 < \alpha(0.05) = 0.0253$ by Welch's $t$ test. (B) $CB6F_1$ mice were injected with the anti-asialoGM1 Ab as described previously (16) and inoculated with 150 SFFU of FV. Percentages of NK cells expressing both DX5 and NK-1.1 markers among spleen cells were monitored by multicolor flow cytometry as shown in Fig. 1, inset, and percentages of $gp70^+$ cells were determined by the specific binding of Ab 720 at the indicated time points. Data shown here are mean ± SEM calculated with values obtained from 5 to 12 animals per group at each time point. Comparisons were made between the anti-asialoGM1-treated and control groups: *, $P < 0.03$; †, $P < 0.005$ by Welch's $t$ test. (C) Survival of anti-asialoGM1-treated animals ($n = 6$) after FV infection compared with that of control mice given normal rabbit serum ($n = 6$). As $CB6F_1$ mice are highly susceptible to FV and most died within 60 days after inoculation with as low as 15 SFFU in a previous experiment (16), a slightly lower dose of 50 SFFU was selected here in an attempt to detect the possibly increased susceptibility in NK-depleted mice. Two survival curves were compared by Mantel-Cox log-rank test: *, $P = 0.026$. (D and E) Groups of $CB6F_1$ mice were injected with either the RAE-1-bloking Ab (49) or control rat IgG and inoculated with 150 (D) or 50 SFFU (E) of FV. Spleen infectious centers were enumerated at PID 6 as described previously (19, 44–47), separate groups were killed at PID 13, and their spleen weights measured. The slightly reduced dose was utilized for the experiment shown in panel E, for the sake of consistency with the survival experiment described in the legend to panel C. Each symbol represents a datum from an individual mouse. †, $P < 0.0005$ by Welch's $t$ test; **, $P = 0.0028$ by Student's $t$ test.

deficient mice, a large proportion of $TER\text{-}119^+$ cells were infected and expressed gp70; however, unlike the $TER\text{-}119^+$ $gp70^+$ cells in the same gene-targeted mice infected with FV complex, these cells showed only a slight increase in RAE-1 expression (Fig. 7A, arrows). Similar effects of the absence of the SFFV component on the expression of RAE-1 in erythroid cells were more evidently observed with BAFF-R-deficient mice: $TER\text{-}119^+$ cells were infected with F-MuLV and expressed gp70, but unlike the same population of erythroid cells in FV-infected mice, these cells did not show a marked increase in the expression of RAE-1 proteins on their surfaces (Fig. 7A, orange dots). On the other hand, $B220^+$ B cells in F-MuLV-infected *BAFF-R*$^{-/-}$ mice (Fig. 7A, blue dots) showed increased expression of RAE-1 as observed upon FV infection.

To further confirm the above differences in RAE-1 expression levels between erythroid cells and B lymphocytes upon FV and F-MuLV infections, $TER\text{-}119^+$ and $B220^+$ cells were gated and their expression levels of RAE-1 proteins were compared between $gp70^+$ and $gp70^-$ populations. When infected with the FV complex, the $gp70^+$ populations of both $TER\text{-}119^+$ and $B220^+$ cells expressed significantly higher levels of RAE-1 than the corresponding $gp70^-$ cells in both APOBEC3- and BAFF-R-deficient animals (Fig. 7B). The average levels of RAE-1 expression on $gp70^+$ cells were 2.69 ± 0.12 and 3.28 ± 0.26 times higher than those on $gp70^-$ cells among $TER\text{-}119^+$ and $B220^+$ cell populations, respectively, in FV-infected BAFF-R-deficient mice. On the other hand, although levels of RAE-1 expression between $gp70^+$ and $gp70^-$ populations were significantly different, $gp70^+$ cells among $TER\text{-}119^+$ erythroid cells in F-MuLV-infected BAFF-R-deficient mice expressed on their surfaces a level of RAE-1 proteins only 1.47 ± 0.06 times higher than that of $gp70^-$ cells, while RAE-1 expression in the $gp70^+$ population of $B220^+$ B lymphocytes became even higher than that observed with FV-infected mice. In fact, the average level of RAE-1 expression on $gp70^+$ cells among $B220^+$ cells was 4.54 ± 0.13 times higher than that on $gp70^-$ cells. Thus, these results indicate that SFFV is required for highly increased expression of RAE-1 on $TER\text{-}119^+$ erythroid cells, while replication of F-MuLV alone induces increased RAE-1 expression in $B220^+$ B cells.

## DISCUSSION

As we have shown here, $NKG2D^+$ NK cells expanded in the spleen and the levels of RAE-1 expression became preferentially higher on the surfaces of viral gp70-expressing cells in FV-infected mice. Although we have not tested all known

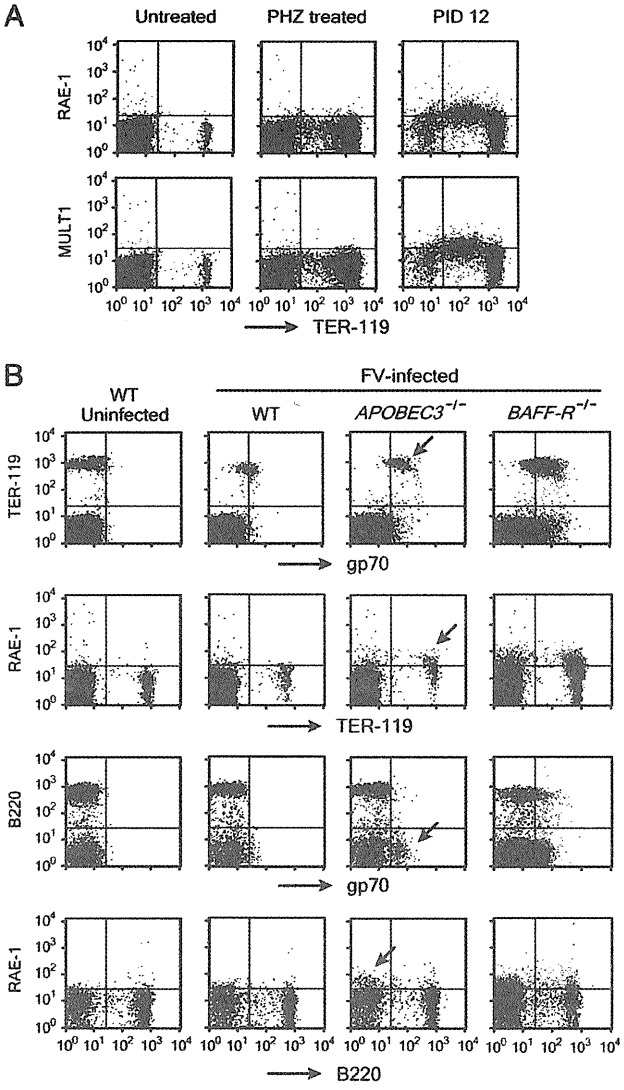


FIG. 6. RAE-1 expression on erythroid progenitor cells is induced by FV infection, not by erythropoiesis. (A) Representative dot plots showing the expression of NK receptor ligand proteins on the surfaces of nucleated spleen cells in phenylhydrazine-treated $CB6F_1$ mice. $CB6F_1$ mice were either injected with 1.2 mg/mouse PHZ on days 0 and 1 or inoculated with 150 SFFU FV on day 0, and at least 4 mice were killed on day 5 or day 12, respectively, to remove the spleen. Multicolor flow cytometric analyses were performed on nucleated cells with each indicated Ab. Demarcation lines were set based on the fluorescence levels observed by incubating the cells with isotype control Ab. Patterns observed with all 4 mice for each experimental group were consistent with those shown here. (B) Representative dot plots showing the expression of viral gp70, RAE-1, erythroid marker TER-119, and B-cell marker B220 on the surfaces of nucleated spleen cells in FV-infected B6 mice lacking an FV-resistance factor. As *Fv2*$^{r/r}$ mice were utilized, they were infected with $5 \times 10^4$ SFFU of FV complex, and 4 to 5 mice for each group were killed to remove the spleen. Flow cytometric analyses were performed as described in the legend to Fig. 3. Representative data obtained at PID 10 are shown here. In panel A, red dots, TER-119$^{Lo}$ gp70$^{Hi}$ cells. In panel B, red dots, TER-119$^-$ gp70$^+$ cells; orange dots, TER-119$^+$ gp70$^+$ cells; purple dots, B220$^-$ gp70$^+$ cells; blue dots, B220$^+$ gp70$^+$ cells in FV-infected *BAFF-R*$^{-/-}$ mice.

ligands for NK cell receptors, the nearly complete abrogation of the killing activities against F-MuLV-induced FBL-3 target cells exerted by DX5$^+$ cells purified from FV-infected $CB6F_1$ mice *in vitro* and the significant increase in the number of FV infectious centers *in vivo* in the presence of the NKG2D-blocking Ab clearly indicate that the NKG2D receptor is involved primarily in the recognition and elimination of infected erythroid cells in FV-inoculated animals. Further, although the levels of induction of RAE-1 proteins on the surfaces of gp70$^+$ erythroid cells were relatively low, as detectable by flow cytometry with the currently utilized Ab, and the same gp70$^+$ TER-119$^{Lo}$ cells retained Qa-1$^b$ molecules on their surfaces, the induced RAE-1 proteins are apparently sufficient to induce the elimination of FV-infected erythroid cells *in vivo*, as the administration of the RAE-1-blocking Ab resulted in significantly increased numbers of infectious centers and more pronounced splenomegaly after FV inoculation. In this regard, FBL-3 cells were killed efficiently by purified NK cells despite their expression of Qa-1$^b$ on the surfaces. Thus, NKG2D–RAE-1 interactions are involved in the elimination of virus-infected cells in the early stages of FV infection *in vivo*. These results are consistent with the previous finding that overexpression of VEGF-A paradoxically resulted in delayed development of FV-induced leukemia, probably due partly to enhanced NK cell activities in the transgenic mice (4).

The mechanisms by which FV infection upregulates the expression of RAE-1 molecules in erythroid progenitor cells and B lymphocytes are currently unknown. Several cytokines, including IFN-γ, have been shown to upregulate the expression of these retinoid-inducible genes (8, 49), and we have demonstrated in the present study that IFN-γ augments the expression of *Raet1* genes in F-MuLV-induced leukemia cells. As the production of IFN-γ in the spleens of FV-infected mice has been detected at as early as 5 days after virus inoculation (31), the induction of *Raet1* gene expression in FV-infected cells might be mediated by IFN-γ. However, as higher levels of RAE-1 proteins were expressed preferentially on gp70$^+$ cells, it is unlikely that cytokine-mediated induction, which should work on both FV-infected and uninfected cells in the spleen, is responsible mainly for the increased levels of RAE-1 protein expression on FV-infected cells. The lack of increased RAE-1 expression on TER-119$^{Lo}$ cells in PHZ-injected mice also indicates the presence of a virus-specific, rather than a differentiation- or growth-associated, mechanism of RAE-1 induction. In this regard, infection of mouse primary B lymphocytes with highly leukemogenic Abelson MuLV induces the expression of activation-induced cytidine deaminase (AID), and the genotoxic action of AID leads to upregulation of NKG2D ligands on infected cell surfaces (11). HIV-1 Vpr is also known to upregulate the expression of NKG2D ligands on cell surfaces (35), and the above Vpr-induced upregulation of NKG2D ligand expression has been shown to be mediated through the DNA damage response (48). Thus, it is tempting to speculate that repeated proviral integrations into the erythroid progenitor cells that are facilitated in the presence of SFFV-induced growth potentiation may cause DNA damage and the resultant upregulation of RAE-1 expression in FV-infected erythroid cells.

Taking advantage of known FV-resistant host factors (5, 12, 25, 27, 46, 47), we successfully dissected here the effect of

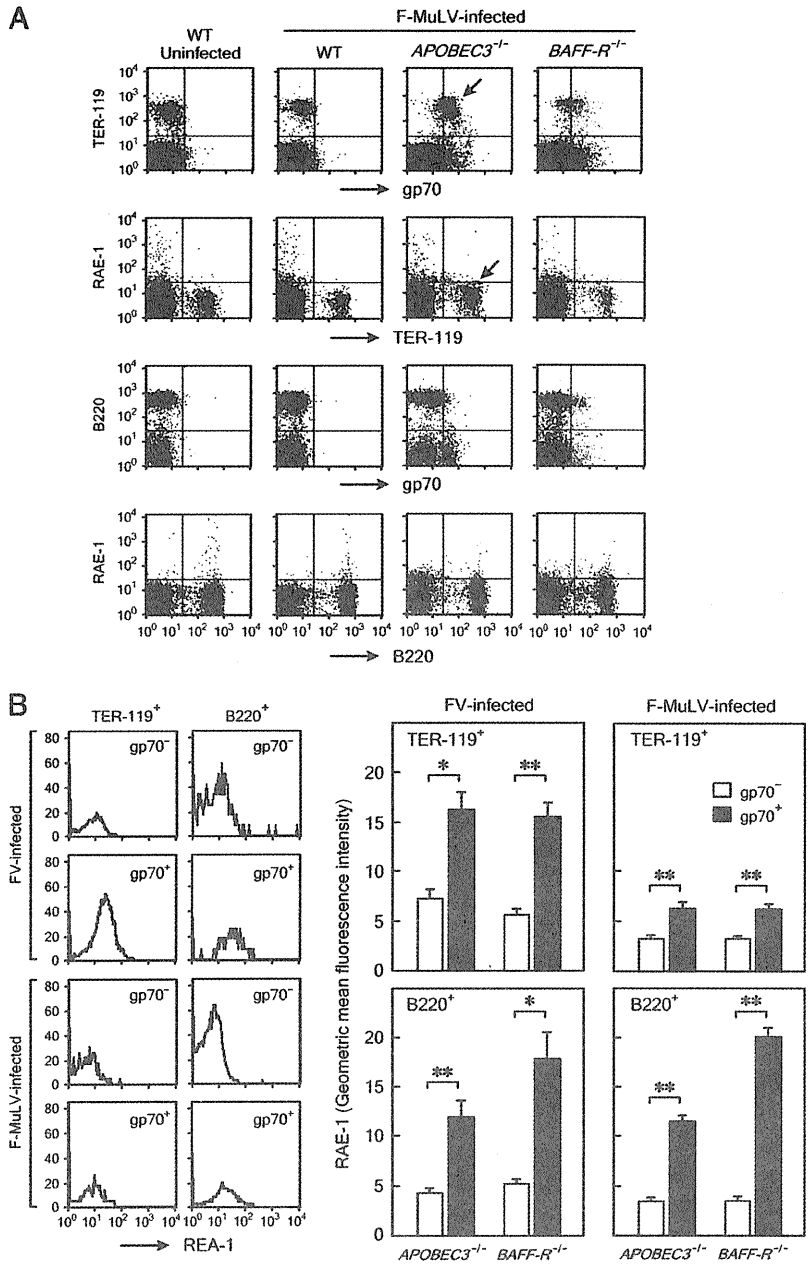


FIG. 7. RAE-1 expression on spleen cells upon infection with F-MuLV alone. (A) Representative dot plots showing the expression of viral gp70, RAE-1 proteins, TER-119, and B220 on the surfaces of nucleated spleen cells in F-MuLV-infected B6 mice lacking an FV resistance factor. Mice were infected with $5 \times 10^4$ fluorescent focus units of F-MuLV (FB-29), and 4 or 5 mice for each group were killed to remove the spleen. Flow cytometric analyses were performed as described for Fig. 3. Representative data obtained at PID 10 are shown here. Arrows, slight increase in RAE-1 expression on the surfaces of TER-119$^+$ gp70$^+$ cells in F-MuLV-infected *APOBEC3*$^{-/-}$ mice. Red dots, TER-119$^-$ gp70$^+$ cells; orange dots, TER-119$^+$ gp70$^+$ cells; purple dots, B220$^-$ gp70$^+$ cells; blue dots, B220$^+$ gp70$^+$ cells in F-MuLV-infected *BAFF-R*$^{-/-}$ mice. (B) Representative histograms on the left show different levels of RAE-1 expression on gp70$^-$ and gp70$^+$ populations of TER-119$^+$ erythroid and B220$^+$ B cells. Averages of GMFI for RAE-1 compared between the gp70$^-$ and gp70$^+$ populations of TER-119$^+$ erythroid cells and B220$^+$ B lymphocytes are shown on the right. Each bar shows mean ± SEM calculated with GMFI data obtained from 4 or 5 mice. *, $P < 0.02$; **, $P < 0.004$ by paired *t* test.

SFFV-induced erythroid cell growth potentiation from that of FV replication on RAE-1 induction in target cells. In fact, FV infection in the absence of massive erythroid cell proliferation still resulted in highly increased RAE-1 expression on TER-119$^+$ erythroid cells in *Fv2*$^r$ B6 mice lacking either APOBEC3 or BAFF-R. Highly increased expression of RAE-1 on infected erythroid as well as B cells in the gene-targeted B6 mice indicates a close correlation between high levels of retroviral rep-

lication and induction of RAE-1 expression on target cells. It should be noted, however, that although B cells expressed similarly increased levels of RAE-1 proteins upon infection with FV complex or with F-MuLV alone, levels of RAE-1 induction on erythroid cells became much higher in the presence of the SFFV component. Thus, in the above conditions of nonrestricted retroviral replication, F-MuLV alone can induce RAE-1 expression in B cells, while SFFV is also required for the induction of high levels of RAE-1 in erythroid cells. In fact, SFFV-induced growth potentiation of infected erythroid cells in the *Fv2*$^s$-possessing CB6F$_1$ mice further enhanced RAE-1 expression on gp70$^+$ erythroblasts, as RAE-1 levels on gp70$^+$ cells in CB6F$_1$ mice were apparently higher than those in the gene-targeted B6 mice (compare fluorescence intensities between Fig. 4 and 7). Nevertheless, the above cell type-associated differences in RAE-1 expression in F-MuLV-infected B6 mice may facilitate further dissection of viral and cellular factors that are involved in retrovirus-induced RAE-1 upregulation.

In the present study, we observed a lag in the increase of TER-119$^+$ erythroblasts until PID 8, followed by an abrupt and massive increase of gp70$^+$ cells in the spleen by PID 12. An abrupt increase in the number of TER-119$^+$ cells in the spleen starting around PID 8 has repeatedly been observed with *Fv2*$^s$-possessing mice (16, 19, 26), which is consistent with a recent finding of two distinctive populations of target cells for FV infection (43). Thus, one population expresses the short-form STK and generates erythropoietin-independent erythroid burst-forming units (BFU-E) in the bone marrow soon after FV infection, while cells of the other population migrate into the spleen as infectious centers, interact with the stromal cells to express bone morphogenic protein 4, and cause the expansion of stress BFU-E. It is tempting to speculate that the cells expressing increased levels of RAE-1 and MULT1 are FV-infected stress BFU-E and that they are susceptible to NK killing. As the depletion of NK cells or the blockade of either NKG2D or RAE-1 resulted in significantly increased FV infectious centers in the spleen at as early as PID 6, followed by significantly more pronounced splenomegaly and earlier death, it is also possible that NK cells are restricting the migration of CD31$^+$ Kit$^+$ CD41$^+$ Sca1$^-$ Lin$^-$ infectious center cells into the spleen. In fact, immunization of mice with the gp70-derived Th-cell epitope suppressed the above abrupt expansion of TER-119$^+$ cells in the spleen that otherwise started from PID 8 (16, 19, and 26), and this vaccine effect was abrogated by depletion of NK cells (16), indicating that Th cell-mediated activation of NK cells may have suppressed the migration of FV infectious centers from bone marrow. Thus, this model may also shed light on basic mechanisms through which the migration of committed erythroid progenitor cells from bone marrow to the spleen might be regulated by NK cell functions.

## ACKNOWLEDGMENTS

This work was supported in part by grants-in-aid from the Ministry of Education, Culture, Sports, Science, and Technology of Japan, including the High-Tech Research Center, Medico-Technical Cooperation, and Anti-Aging Center grants, those from the Ministry of Health, Labor, and Welfare of Japan for Research on HIV/AIDS, and those from the Japan Health Sciences Foundation. The use of radioisotopes, animal experiments, and flow cytometric analyses were supported by members of the Central Research Facilities, Kinki University School of Medicine.

We are grateful to J. Brian Dowell for critically reading and correcting the manuscript and to Yoshiko Ito, Department of Respiratory Medicine and Allergology, Kinki University School of Medicine, for her help in operating the AutoMACS.

## REFERENCES

1. **Alter, G., et al.** 2007. Evolution of innate and adaptive effector cell functions during acute HIV-1 infection. J. Infect. Dis. **195:**1452–1460.
2. **Arase, H., T. Saito, J. H. Phillips, and L. L. Lanier.** 2001. Cutting edge: the mouse NK cell-associated antigen recognized by DX5 monoclonal antibody is CD49b ($\alpha_2$ integrin, very late antigen-2). J. Immunol. **167:**1141–1144.
3. **Azakami, K., et al.** 2009. Severe loss of invariant NKT cells exhibiting anti-HTLV-1 activity in patients with HTLV-1-associated disorders. Blood **114:**3208–3215.
4. **Cervi, D., et al.** 2007. Enhanced natural-killer cell and erythropoietic activities in VEGF-A-overexpressing mice delay F-MuLV-induced erythroleukemia. Blood **109:**2139–2146.
5. **Chesebro, B., M. Miyazawa, and W. J. Britt.** 1990. Host genetic control of spontaneous and induced immunity to Friend murine retrovirus infection. Annu. Rev. Immunol. **8:**477–499.
6. **Costello, R. T., C. Fauriat, S. Sinori, E. Marcenaro, and D. Olive.** 2004. NK cells: innate immunity against hematopoietic malignancies? Trends Immunol. **26:**328–333.
7. **Dittmer, U., et al.** 2001. Role of interleukin-4 (IL-4), IL-12, and gamma interferon in primary and vaccine-primed immune responses to Friend retroviral infection. J. Virol. **75:**654–660.
8. **Faria, P. A., et al.** 2005. VSV disrupts the Rae1/mrnp41 mRNA nuclear export pathway. Mol. Cell **17:**93–102.
9. **Gaudieri, S., et al.** 2005. Killer immunoglobulin-like receptors and HLA act both independently and synergistically to modify HIV disease progression. Genes Immun. **6:**683–690.
10. **Giavedoni, L. D., M. C. Velasquillo, L. M. Parodi, G. B. Hubbard, and V. L. Hodora.** 2000. Cytokine expression, natural killer cell activation, and phenotypic changes in lymphoid cells from rhesus macaques during acute infection with pathogenic simian immunodeficiency virus. J. Virol. **74:**1648–1657.
11. **Gourzi, P., T. Leonova, and F. N. Papavasiliou.** 2006. A role for activation-induced cytidine deaminase in the host response against a transforming retrovirus. Immunity **24:**779–786.
12. **Hasenkrug, K. J., and B. Chesebro.** 1997. Immunity to retroviral infection: the Friend virus model. Proc. Natl. Acad. Sci. U. S. A. **94:**7811–7816.
13. **Ho, E. L., et al.** 2002. Costimulation of multiple NK cell activation receptors by NKG2D. J. Immunol. **169:**3667–3675.
14. **Howcroft, T. K., and D. S. Singer.** 2003. Expression of nonclassical MHC class Ib genes: comparison of regulatory elements. Immunol. Res. **27:**1–30.
15. **Iannello, A., O. Debbeche, S. Samarani, and A. Ahmad.** 2008. Antiviral NK cell responses in HIV infection. I. NK cell receptor genes as determinants of HIV resistance and progression to AIDS. J. Leuko. Biol. **84:**1–26.
16. **Iwanami, N., A. Niwa, Y. Yasutomi, N. Tabata, and M. Miyazawa.** 2001. Role of natural killer cells in resistance against Friend retrovirus-induced leukemia. J. Virol. **75:**3152–3163.
17. **Jamieson, A. M., et al.** 2002. The role of the NKG2D immunoreceptor in immune cell activation and natural killing. Immunity **17:**19–29.
18. **Kabat, D.** 1989. Molecular biology of Friend viral erythroleukemia. Curr. Top. Microbiol. Immunol. **148:**1–42.
19. **Kawabata, H., et al.** 2006. Peptide-induced immune protection of CD8$^+$ T cell-deficient mice against Friend retrovirus-induced disease. Int. Immunol. **18:**183–198.
20. **Kina, T., et al.** 2000. The monoclonal antibody TER-119 recognizes a molecule associated with glycophorin A and specifically marks the late stages of murine erythroid lineage. Br. J. Haematol. **109:**280–287.
21. **Kottilil, S., et al.** 2003. Innate immunity in human immunodeficiency virus infection: effect of viremia on natural killer cell function. J. Infect. Dis. **187:**1038–1045.
22. **Maier, L. M., et al.** 2008. NKG2D–RAE-1 receptor-ligand variation does not account for the NK cell defect in Nonobese diabetic mice. J. Immunol. **181:**7073–7080.
23. **Martin, M. P., et al.** 2002. Epistatic interaction between KIR3DS1 and HLA-B delays the progression to AIDS. Nat. Genet. **31:**429–434.
24. **Martin, M. P., et al.** 2007. Innate partnership of HLA-B and KIR3DL1 subtypes against HIV-1. Nat. Genet. **39:**733–740.
25. **Miyazawa, M.** 2004. Host genes that influence immune and non-immune resistance mechanisms against retroviral infections. Rec. Res. Dev. Virol. **6:**105–118.
26. **Miyazawa, M., et al.** 1995. Immunization with a single T helper cell epitope abrogates Friend virus-induced early erythroid proliferation and prevents late leukemia development. J. Immunol. **155:**748–758.
27. **Miyazawa, M., S. Tsuji-Kawahara, and Y. Kanari.** 2008. Host genetic factors that control immune responses to retrovirus infections. Vaccine **26:**2981–2996.

28. **Ney, P. A., and A. D. D'Andrea.** 2000. Friend erythroleukemia revisited. Blood **96**:3675–3680.
29. **Ogasawara, K., et al.** 2004. NKG2D blockade prevents autoimmune diabetes in NOD mice. Immunity **20**:757–767.
30. **Ogasawara, K., and L. L. Lanier.** 2005. NKG2D in NK and T cell-mediated immunity. J. Clin. Immunol. **25**:534–540.
31. **Peterson, K. E., M. Iwashiro, K. J. Hasenkrug, and B. Chesebro.** 2000. Major histocompatibility complex class I gene controls the generation of gamma interferon-producing $CD4^+$ and $CD8^+$ T cells important for recovery from Friend retrovirus-induced leukemia. J. Virol. **74**:5363–5367.
32. **Peterson, K. E., I. Stromnes, R. Messer, K. Hasenkrug, and B. Chesebro.** 2002. Novel role of $CD8^+$ T cells and major histocompatibility complex class I genes in the generation of protective $CD4^+$ Th1 responses during retrovirus infection in mice. J. Virol. **76**:7942–7948.
33. **Pradet-Balade, B., C. Leberbauer, N. Schweifer, and F. Boulmé.** 2010. Massive translational repression of gene expression during mouse erythroid differentiation. Biochim. Biophys. Acta **1799**:630–641.
34. **Ravet, S., et al.** 2007. Distinctive NK-cell receptor repertoires sustain high-level constitutive NK-cell activation in HIV-exposed uninfected individuals. Blood **109**:4296–4305.
35. **Richard, J., S. Sindhu, T. N. Pham, J. P. Belzile, and E. A. Cohen.** 2010. HIV-1 Vpr up-regulates expression of ligands for the activating NKG2D receptor and promotes NK cell-mediated killing. Blood **115**:1354–1363.
36. **Robertson, M. N., et al.** 1991. Production of monoclonal antibodies reactive with a denatured form of the Friend murine leukemia virus gp70 envelope protein: use in a focal infectivity assay, immunohistochemical studies, electron microscopy and Western blotting. J. Virol. Methods **34**:255–271.
37. **Sasaki, Y., S. Casola, J. L. Kutok, K. Rajewsky, and M. Schmidt-Supprian.** 2004. TNF family member B cell-activating factor (BAFF) receptor-dependent and -independent roles for BAFF in B cell physiology. J. Immunol. **173**:2245–2252.
38. **Scott-Algara, D., et al.** 2003. Increased NK cell activity in HIV-1-exposed but uninfected Vietnamese intravenous drug users. J. Immunol. **171**:5663–5667.
39. **Seaman, W. E.** 2000. Natural killer cells and natural killer T cells. Arthritis Rheum. **43**:1204–1217.
40. **Sieff, C., et al.** 1982. Changes in cell surface antigen expression during hemopoietic differentiation. Blood **60**:703–713.
41. **Slifka, M. K., R. R. Pagarigan, and J. L. Whitton.** 2000. NK markers are expressed on a high percentage of virus-specific $CD8^+$ and $CD4^+$ T cells. J. Immunol. **164**:2009–2015.
42. **Stromnes, I. M., et al.** 2002. Temporal effects of gamma interferon deficiency on the course of Friend retrovirus infection in mice. J. Virol. **76**:2225–2232.
43. **Subramanian, A., et al.** 2008. Friend virus utilizes the BMP4-dependent stress erythropoiesis pathway to induce erythroleukemia. J. Virol. **82**:382–393.
44. **Sugahara, D., S. Tsuji-Kawahara, and M. Miyazawa.** 2004. Identification of a protective $CD4^+$ T-cell epitope in $p15^{gag}$ of Friend murine leukemia virus and role of the MA protein targeting the plasma membrane in immunogenicity. J. Virol. **78**:6322–6334.
45. **Takamura, S., et al.** 2010. Premature terminal exhaustion of Friend virus-specific effector $CD8^+$ T cells by rapid induction of multiple inhibitory receptors. J. Immunol. **184**:4696–4707.
46. **Takeda, E., et al.** 2008. Mouse APOBEC3 restricts Friend leukemia virus infection and pathogenesis in vivo. J. Virol. **82**:10998–11008.
47. **Tsuji-Kawahara, S., et al.** 2010. Persistence of viremia and production of neutralizing antibodies differentially regulated by polymorphic *APOBEC3* and *BAFF-R* loci in Friend virus-infected mice. J. Virol. **84**:6082–6095.
48. **Ward, J., et al.** 2009. HIV-1 Vpr triggers natural killer cell-mediated lysis of infected cells through activation of the ATR-mediated DNA damage response. PLoS Pathog. **5**:e1000613.
49. **Yokoyama, W. M., and B. F. M. Plougastel.** 2003. Immune functions encoded by the natural killer gene complex. Nat. Rev. Immunol. **3**:304–316.
50. **Zhang, J., M. Socolovsky, A. W. Gross, and H. F. Lodish.** 2003. Role of Ras signaling in erythroid differentiation of mouse fetal liver cells: functional analysis by a flow cytometry-based novel culture system. Blood **102**:3938–3946.
51. **Zhou, R., H. Wei, R. Sun, J. Zhang, and Z. Tian.** 2007. NKG2D recognition mediates Toll-like receptor 3 signaling-induced breakdown of epithelial homeostasis in the small intestines of mice. Proc. Natl. Acad. Sci. U. S. A. **104**:7512–7515.

Molecular Immunology 48 (2011) 497–504

Contents lists available at ScienceDirect

Molecular Immunology

journal homepage: www.elsevier.com/locate/molimm

# Strain-to-strain difference of V protein of measles virus affects MDA5-mediated IFN-β-inducing potential

Hiromi Takaki[1], Yumi Watanabe[1], Masashi Shingai[2], Hiroyuki Oshiumi, Misako Matsumoto, Tsukasa Seya*

*Department of Microbiology and Immunology, Graduate School of Medicine, Hokkaido University, Kita-ku, Sapporo 060-8638, Japan*

ARTICLE INFO

*Article history:*
Received 22 June 2010
Received in revised form 7 October 2010
Accepted 12 October 2010
Available online 10 November 2010

*Keywords:*
Measles virus
V protein
MDA5
IRF-3
Interferon-beta

ABSTRACT

Laboratory-adapted and vaccine strains of measles virus (MV) induce type I interferon (IFN) in infected cells to a far greater extent than wild-type strains. We investigated the mechanisms for this differential type I IFN production in cells infected with representative MV strains. The overexpression of the wild-type V protein suppressed melanoma differentiation-associated gene 5 (MDA5)-induced IFN-β promoter activity, while this was not seen in A549 cells expressing CD150 transfected with the V protein of the vaccine strain. The V proteins of the wild-type also suppressed poly I:C-induced IFN regulatory factor 3 (IRF-3) dimerization. The V proteins of the wild-type and vaccine strain did not affect retinoic acid-inducible gene 1 (RIG-I)- or toll-IL-1R homology domain-containing adaptor molecule 1 (TICAM-1)-induced IFN-β promoter activation. We identified an amino acid substitution of the cysteine residue at position 272 (which is conserved among paramyxoviruses) to an arginine residue in the V protein of the vaccine strain. Only the V protein possessing the 272C residue binds to MDA5. The mutation introduced into the wild-type V protein (C272R) was unable to suppress MDA5-induced IRF-3 nuclear translocation and IFN-β promoter activation as seen in the V proteins of the vaccine strain, whereas the mutation introduced in the vaccine strain V protein (R272C) was able to inhibit MDA5-induced IRF-3 and IFN-β promoter activation. The other 6 residues of the vaccine strain V sequence inconsistent with the authentic sequence of the wild-type V protein barely affected the IRF-3 nuclear translocation. These data suggested that the structural difference of vaccine MV V protein hampers MDA5 blockade and acts as a nidus for the spread/amplification of type I IFN induction. Ultimately, measles vaccine strains have two modes of IFN-β-induction for their attenuation: V protein mutation and production of defective interference (DI) RNA.

© 2010 Elsevier Ltd. All rights reserved.

## 1. Introduction

Innate immunity is the first line of defense against virus infection, and the most powerful antiviral agent possessed by the host immune system is interferon (IFN). Expression of type I IFN in host cells induces a set of IFN-inducible genes which efficiently suppress viral replication and spread (Pichlmair and Reis, 2007). Host cells usually terminate virus replication in response to IFN induction. Recent studies elucidated the mechanism by which type I IFN is induced and found that it senses virus patterns such as 5′-triphosphate (5′-3P) and stem-loops or double-stranded RNA (dsRNA) (Takeuchi and Akira, 2008). dsRNA specifically is present in several forms: viral genomes, single-stranded RNA virus replication intermediates, DNA virus symmetrical transcription products, defective viral particles and debris from lysed cells (Bowie and Fitzgerald, 2007). These viral products all present patterns that activate the IFN system. In fact, extracellular dsRNA is sensed by endosomal Toll-like receptor 3 (TLR3), and intracellular dsRNA is detected by cytoplasmic RNA helicase retinoic acid-inducible gene 1 (RIG-I) and melanoma differentiation-associated gene 5 (MDA5) (Takeuchi and Akira, 2008). TLR3 recruits the adaptor, toll-IL-1R homology domain-containing adaptor molecule 1 (TICAM-1, also named TRIF) (Oshiumi et al., 2003). RIG-I and MDA5 signal through IFN-β promoter stimulator 1 (IPS-1). These adaptor molecules activate kinase TANK-binding kinase I (TBK1), inhibitor of κB kinase ε (IKKε) and NAK-associated protein 1 (NAP-1) (Sasai et al., 2006a). These complexes then phosphorylate IFN regulatory factor 3 (IRF-

* Corresponding author at: Department of Microbiology and Immunology, Graduate School of Medicine, Hokkaido University, Kita 15, Nishi 7, Kita-ku, Sapporo 060-8638, Japan. Tel.: +81 11 706 7866; fax: +81 11 706 7866.
*E-mail address:* seya-tu@pop.med.hokudai.ac.jp (T. Seya).
[1] First two authors equally contributed to this work.
[2] Present address: Laboratory of Molecular Microbiology, National Institute of Allergy and Infectious Diseases, National Institutes of Health, Bethesda, MD 20892.

0161-5890/$ – see front matter © 2010 Elsevier Ltd. All rights reserved.
doi:10.1016/j.molimm.2010.10.006